

**Clouds and the Earth's Radiant Energy System
(CERES)**

Data Management System

DRAFT ES-8 Collection Guide

**Release 3
Version 4**

Primary Authors

Lee-hwa Chang, John L. Robbins

Science Applications International Corporation (SAIC)
One Enterprise Parkway, Suite 300
Hampton, VA 23666-5845

Richard N. Green, James F. Kibler

NASA Langley Research Center
Climate Science Branch
Science Directorate
Building 1250
21 Langley Boulevard
Hampton, VA 23681-2199

January 2003

Document Revision Record

The Document Revision Record contains information pertaining to approved document changes. The table lists the date the Software Configuration Change Request (SCCR) was approved, the Release and Version Number, the SCCR number, a short description of the revision, and the revised sections. The document authors are listed on the cover. The Head of the CERES Data Management Team approves or disapproves the requested changes based on recommendations of the Configuration Control Board.

Document Revision Record

SCCR Approval Date	Release/Version Number	SCCR Number	Description of Revision	Section(s) Affected
01/10/01	R3V3	236	• Added maximum file size with HDF compression to the ES-8 Product Summary Table.	5.0
			• Changed all references to number of records from 13091 to 13092.	5.0, 5.2, 5.3, & 15.0
			• Switched the first and second dimensions of the SDS Elements so that the first dimension reflects the number of 6.6-second records contained in the data-day.	5.2
			• Updated format to comply with standards.	All
07/03/02	R3V4	369	• Renamed EOS-PM to Aqua.	All
			• Renamed DAAC to ASDC.	All
			• The launch and data start date for the Aqua spacecraft was supplied.	Table 4-2
			• ES-8 Vdata, ES8-V21 (Spectral Response Functions), definition was added.	4.3.1
			• Range for LW TOA flux was changed to 50 .. 450.	Table 5-3
			• Added ES-8 Spectral Response Functions Vdata.	Table 5-4
			• Corrected ES8-V19 and ES8-V20 parameter names to reflect "at observation".	Table 5-4
			• Term-20, Spectral Correction, was added.	15.0
			• Acronym, EOS PM, was added.	16.1
			• Note-6, Spectral Correction Algorithm, was added.	8.0
			• Detector Time Constants for FM3 and FM4 were added.	Table 8-2
			• Updated format to comply with standards.	All

Document Revision Record

SCCR Approval Date	Release/Version Number	SCCR Number	Description of Revision	Section(s) Affected
07/03/02	R3V4	369	<ul style="list-style-type: none">• The CERES Top Level Data Flow Diagram was modified. (5/29/2003).• This document was converted from FrameMaker to Word. (06/20/2008)• The CERES Top Level Data Flow Diagram was modified. (06/20/2008)• Updated Website links. Some were modified to new sites and some were unlinked as the sites no longer exist. (06/19/2013)	1.3 All Fig. 1-1 Secs. 7.0 & 14.0

Preface

The Clouds and the Earth's Radiant Energy System (CERES) Data Management System supports the data processing needs of the CERES Science Team research to increase understanding of the Earth's climate and radiant environment. The CERES Data Management Team works with the CERES Science Team to develop the software necessary to implement the science algorithms. This software, being developed to operate at the Langley Atmospheric Sciences Data Center (ASDC), produces an extensive set of science data products.

The Data Management System consists of 12 subsystems; each subsystem represents one or more stand-alone executable programs. Each subsystem executes when all of its required input data sets are available and produces one or more archival science products.

This Collection Guide is intended to give an overview of the science product along with definitions of each of the parameters included within the product. The document has been reviewed by the CERES Working Group teams responsible for producing the product and by the Working Group Teams who use the product.

Acknowledgment is given to Tammy O. Ayers and Thanh Duong of Science Applications International Corporation (SAIC) for their support in the preparation of this document.

TABLE OF CONTENTS

<u>Section</u>	<u>Page</u>
Document Revision Record	ii
Preface.....	iv
Summary	1
1.0 Collection Overview	2
1.1 Collection Identification.....	2
1.2 Collection Introduction	2
1.3 Objective/Purpose	2
1.1 Summary of Parameters	5
1.2 Discussion	5
1.3 Related Collections	5
2.0 Investigators.....	6
2.1 Title of Investigation	6
2.2 Contact Information	6
3.0 Origination	7
4.0 Data Description	8
4.1 Spatial Characteristics	8
4.1.1 Spatial Coverage	8
4.1.2 Spatial Resolution	8
4.2 Temporal Characteristics.....	8
4.2.1 Temporal Coverage.....	8
4.2.2 Temporal Resolution.....	9
4.3 Parameter Definitions.....	9
4.3.1 ES-8 V data	9
4.3.2 ES-8 Scientific Data Definitions.....	14

TABLE OF CONTENTS

<u>Section</u>	<u>Page</u>
4.4 Fill Values	28
4.5 Sample Data File	29
5.0 Data Organization	30
5.1 Data Granularity	31
5.2 ES-8 HDF Scientific Data Sets (SDS)	31
5.3 ES-8 HDF Vertex Data (Vdata)	32
5.4 Metadata	33
6.0 Theory of Measurements and Data Manipulations	34
6.1 Theory of Measurements.....	34
6.2 Data Processing Sequence.....	34
6.3 Special Corrections/Adjustments	34
7.0 Errors.....	35
7.1 Quality Assessment	35
7.2 Data Validation by Source	35
8.0 Notes	36
Note-1 Conversion of Julian Date to Calendar Date	36
Note-2 Colatitude and Longitude of Nadir	38
Note-3 CERES Point Spread Function	39
Note-4 Definition of Angular Distribution Models (ADM)	44
Note-5 Maximum Likelihood Estimator (MLE) of Scene Type	45
Note-6 Spectral Correction Algorithm	46
9.0 Application of the Data Set.....	49
10.0 Future Modifications and Plans	50
11.0 Software Description	51

TABLE OF CONTENTS

<u>Section</u>	<u>Page</u>
12.0 Contact Data Center/Obtain Data	52
13.0 Output Products and Availability.....	53
14.0 References.....	54
15.0 Glossary of Terms.....	55
16.0 Acronyms and Units	60
16.1 CERES Acronyms.....	60
16.2 CERES Units.....	62
17.0 Document Information.....	64
17.1 Document Creation Date - May 15, 1998	64
17.2 Document Review Date -	64
17.3 Document Revision Date	64
17.4 Document ID	64
17.5 Citation.....	64
17.6 Redistribution of Data	64
17.7 Document Curator	64
18.0 Index	65
Appendix A CERES Metadata.....	A-1

LIST OF FIGURES

<u>Figure</u>	<u>Page</u>
Figure 1-1. CERES Top Level Data Flow Diagram.....	4
Figure 4-1. Colatitude and Longitude.....	12
Figure 4-2. Viewing Angles at TOA.....	16
Figure 8-1. Scanner Footprint.....	40
Figure 8-2. Optical FOV	41
Figure 8-3. TRMM Angular Bin Weights	44
Figure 8-4. ERBE Scene Identification Algorithm.....	46
Figure 8-5. CERES TRMM Spectral Response.....	48
Figure 15-1. Cone Angle.....	55
Figure 15-2. Ellipsoidal Model.....	56
Figure 15-3. Normal and short Earth scan profiles for instrument on TRMM platform	57

LIST OF TABLES

<u>Table</u>	<u>Page</u>
Table 3-1. CERES Instruments.....	7
Table 4-1. ES-8 Spatial Coverage.....	8
Table 4-2. CERES Temporal Coverage.....	8
Table 4-3. CERES Orbit Characteristics	9
Table 4-4. ERBE Scene Types.....	20
Table 4-5. Bit Order for Radiometric and FOV Quality Flags	21
Table 4-6. Scanner Operations Flag Word 1 (of 3)	22
Table 4-7. Scanner Operations Flag Word 2 (of 3)	24
Table 4-8. Scanner Operations Flag Word 3 (of 3)	25
Table 4-9. CERES Fill Values	29
Table 5-1. ES-8 Product Summary	30
Table 5-2. ES-8 Product Specific Metadata.....	30
Table 5-3. ES-8 SDS Summary	31
Table 5-4. ES-8 Vdata Summary	32
Table 8-1. Julian Day Number.....	38
Table 8-2. Detector Time Constant (□.seconds).....	42
Table A-1. CERES Baseline Header Metadata.....	A-1
Table A-2. CERES_metadata Vdata.....	A-3

Clouds and the Earth's Radiant Energy System (CERES)

ES-8 Collection Guide

Summary

CERES is a key component of the EOS program. The CERES instrument provides radiometric measurements of the Earth's atmosphere from three broadband channels: a shortwave channel (0.3 - 5 μm), a total channel (0.3 - 200 μm), and an infrared window channel (8 - 12 μm). The CERES instruments are improved models of the ERBE scanner instruments, which operated from 1984 through 1990 on NASA's ERBS and on NOAA's operational weather satellites, NOAA-9 and NOAA-10. The strategy of flying instruments on Sun-synchronous, polar orbiting satellites, such as NOAA-9 and NOAA-10, simultaneously with instruments on satellites that have precessing orbits in lower inclinations, such as ERBS, was successfully developed in ERBE to reduce time sampling errors. CERES continues that strategy by flying instruments on the polar orbiting EOS platforms simultaneously with an instrument on the TRMM spacecraft, which has an orbital inclination of 35 degrees. The TRMM satellite carries one CERES instrument while the Terra and Aqua EOS satellites carry two CERES instruments, one operating in a FAPS mode for continuous Earth sampling and the other operating in a RAPS mode for improved angular sampling.

To preserve historical continuity, some parts of the CERES data reduction use algorithms identical with the algorithms used in ERBE. At the same time, many of the algorithms on CERES are new. To reduce the uncertainty in data interpretation and to improve the consistency between the cloud parameters and the radiation fields, CERES includes cloud imager data and other atmospheric parameters. The CERES investigation is designed to monitor the top-of-atmosphere radiation budget as defined by ERBE, to define the physical properties of clouds, to define the surface radiation budget, and to determine the divergence of energy throughout the atmosphere. The CERES DMS produces products which support research to increase understanding of the Earth's climate and radiant environment.

The ES-8 archival data product was created as an HDF-EOS (See Reference 1) swath data structure and contains a 24-hour, single-satellite, instantaneous view of scanner fluxes at the TOA (See [Term-22](#)) reduced from spacecraft altitude unfiltered radiances using the ERBE scanner Inversion algorithms and the ERBE SW and LW ADMs. The ES-8 also includes the TOT, SW, and WN channel radiometric data; SW, LW, and WN unfiltered radiance values; and the ERBE scene identification for each measurement. These data are organized according to the CERES 3.3-second scan into 6.6-second records. As long as there is one valid scanner measurement within a record, the ES-8 record will be generated.

1.0 Collection Overview

1.1 Collection Identification

The ES-8 filename is

CER_ES8_Sampling-Strategy_Production-Strategy_XXXXXX.YYYYMMDD where

CER	Investigation designation for CERES,
ES8	Product identification for the primary science data product (external distribution),
Sampling-Strategy	Platform, instrument, and imager (e.g., TRMM-PFM-VIRS),
Production-Strategy	Edition or campaign (e.g., At-launch, ValidationR1, Edition1),
XXXXXX	Configuration code for file and software version management,
YYYY	4-digit integer defining data acquisition year,
MM	2-digit integer defining data acquisition month, and
DD	2-digit integer defining the data acquisition day.

1.2 Collection Introduction

The ES-8 data product is a Level-2 archival product that contains a 24-hour, single-satellite, single-instrument, instantaneous view of scanner fluxes at the TOA reduced from spacecraft altitude unfiltered radiances using the ERBE scanner Inversion algorithms and the ERBE SW and LW ADMs.

1.3 Objective/Purpose

The overall science objectives of the CERES investigation are

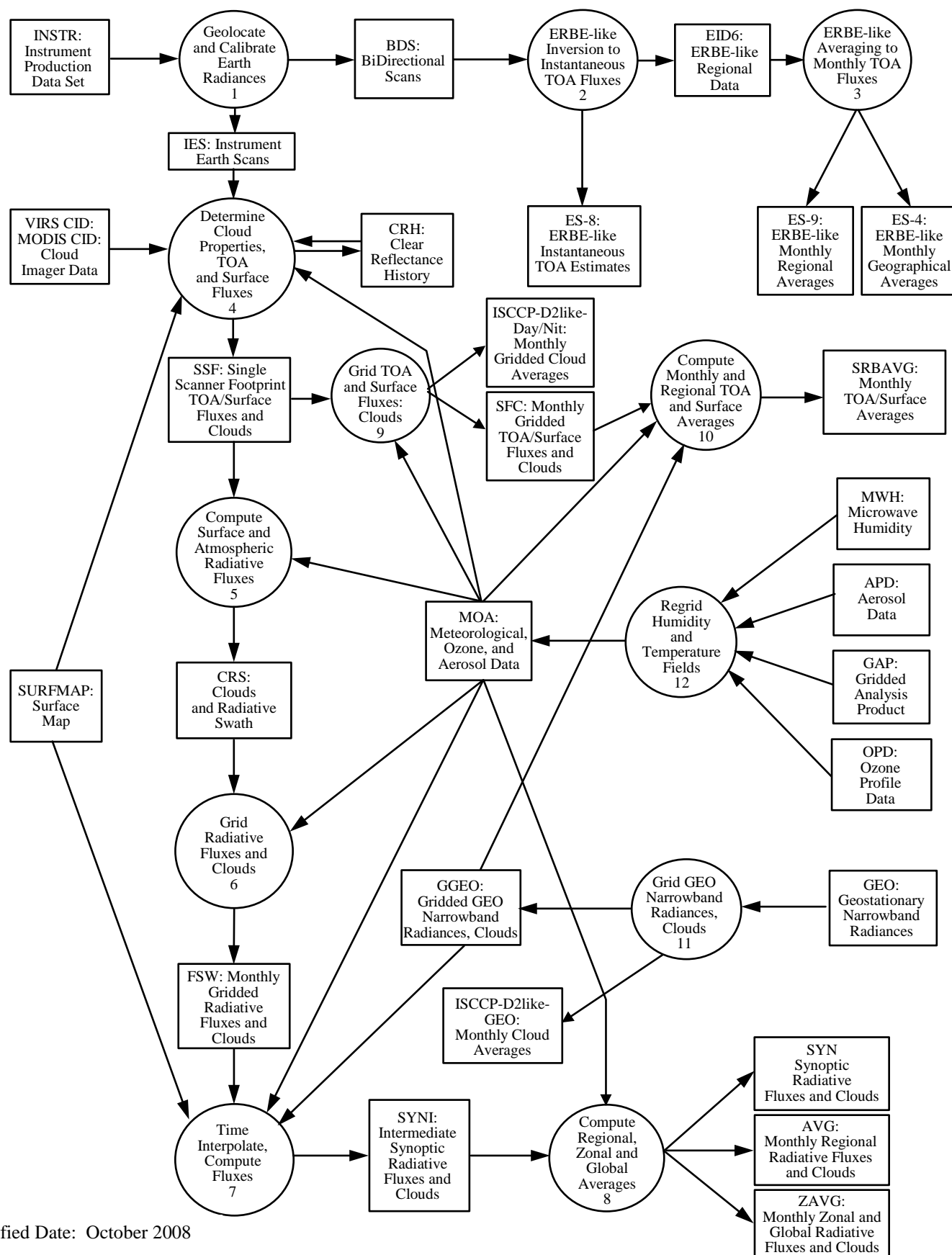
1. For climate change research, provide a continuation of the ERBE radiative fluxes at the TOA that are analyzed using the same techniques used with existing ERBE data.
2. Double the accuracy of estimates of radiative fluxes at the TOA and the Earth's surface from existing ERBE data.
3. Provide the first long-term global estimates of the radiative fluxes within the Earth's atmosphere.
4. Provide cloud property estimates which are consistent with the radiative fluxes from surface to TOA.

The CERES DMS is a software management and processing system which processes CERES instrument measurements and associated engineering data to produce archival science and other data products. The DMS is executed at the LaRC ASDC, which is also responsible for distributing the data products. A high-level view of the CERES DMS is illustrated by the CERES Top Level Data Flow Diagram shown in [Figure 1-1](#).

Circles in the diagram represent algorithm processes called subsystems, which are a logical collection of algorithms that together convert input products into output products. Boxes represent archival products. Two parallel lines represent data stores which are designated as

nonarchival or temporary data products. Boxes or data stores with arrows entering a circle are input sources for the subsystem, while boxes or data stores with arrows exiting the circles are output products.

As shown in [Figure 1-1.](#), the ES-8 product is generated by the CERES ERBE-like Inversion Subsystem (Subsystem 2.0). The input to Subsystem 2.0 is actually the preES-8, a daily file which is generated by an Instrument Subsystem postprocessing program and contains a subset of BDS parameters.



Modified Date: October 2008

Figure 1-1. CERES Top Level Data Flow Diagram

1.1 Summary of Parameters

The ES-8 contains the following kinds of information:

1. Scan-level Data (Vdata Structures)
 - a. Time of Observation (Julian date and time)
 - b. Earth-Sun distance
 - c. Satellite position and velocity and Sun position
2. Measurement-level Data (SDSs)
 - a. Instrument field-of-view (colatitude and longitude)
 - b. Radiometric data (total, shortwave, and window channels))
 - c. Satellite and Sun geometry (viewing zenith, solar zenith, and relative azimuth)
 - d. Unfiltered radiances (shortwave, longwave, and window)
 - e. [TOA](#) fluxes (shortwave and longwave)
 - f. [ERBE](#) scene identification

(1) clear ocean	(5) clear coastal	(9) mostly cloudy ocean
(2) clear land	(6) partly cloudy ocean	(10) mostly cloudy land-desert
(3) clear snow	(7) partly cloudy land-desert	(11) mostly cloudy coastal
(4) clear desert	(8) partly cloudy coastal	(12) overcast

1.2 Discussion

Satellite altitude data from the Instrument Subsystem is processed by the ERBE-like Inversion Subsystem to provide estimates of the radiant flux at the TOA. This inversion process is dependent on several factors, including Earth surface features, the extent of cloudiness, and the relative geometry of the satellite, the Sun, and the measurement FOV. Each radiometric measurement is spectrally corrected (See [Term-20](#)) to give an unfiltered measurement. The observed scene is determined by the ERBE scene identification algorithm based on these unfiltered measurements using ADMs and statistics provided by the Science Team. Estimates of the radiant flux at the TOA are computed based on the scene information, geometrical considerations, and the unfiltered measurements.

1.3 Related Collections

The CERES DMS produces science data products, or collections, for use by the CERES Science Team, the Data Management Team, and for archival at the Langley ASDC. A complete list of collections may be found in the CERES DPC (See Reference 2).

2.0 Investigators

Dr. Bruce A. Wielicki, CERES Principal Investigator

E-mail: B.A.Wielicki@LaRC.NASA.Gov

Telephone: (757) 864-5683

FAX: (757) 864-7996

Mail Stop 420

Atmospheric Sciences Competency

Building 1250

21 Langley Boulevard

NASA Langley Research Center

Hampton, VA 23681-2199

2.1 Title of Investigation

Clouds and the Earth's Radiant Energy System (CERES)

ERBE-like Subsystems (Subsystems 2.0 & 3.0)

2.2 Contact Information

Dr. Kory J. Priestley, Subsystem 2.0 Working Group Chair

E-mail: K.J.Priestley@LaRC.NASA.Gov

Telephone: (757) 864-8147

Dr. Takmeng Wong, Subsystem 2.0 Working Group Science and Validation Advisor

E-mail: Takmeng.Wong@LaRC.NASA.Gov

Telephone: (757) 864-5607

FAX: (757) 864-7996

Mail Stop 420

Atmospheric Sciences Competency

Building 1250

21 Langley Boulevard

NASA Langley Research Center

Hampton, VA 23681-2199

Edward A. Kizer, Subsystem 2.0 Software and Data Management Lead

E-mail: E.A.Kizer@LaRC.NASA.Gov

Telephone: (757) 827-4883

FAX: (757) 864-7996

Science Applications International Corporation (SAIC)

One Enterprise Parkway, Suite 300

Hampton, VA 23666-5845

3.0 Origination

The CERES data originate from CERES instruments on-board either the TRMM, Terra or Aqua EOS Earth-orbiting spacecrafts. [Table 3-1](#) lists the CERES instruments and their host satellites.

Table 3-1. CERES Instruments

Satellite	CERES Instrument	
TRMM	PFM	
Terra	FM1	FM2
Aqua	FM3	FM4

The CERES instrument contains three scanning thermistor bolometer radiometers that measure the radiation in the near-visible through far-infrared spectral region. The shortwave detector measures Earth-reflected and Earth-emitted solar radiation and the window detector measures Earth-emitted longwave radiation in the water vapor window. The total detector measures total Earth-reflected and Earth-emitted radiation. The detectors are coaligned and mounted on a spindle that rotates about the instrument elevation axis. The resolution of the CERES radiometers is usually referenced to the optical FOV (See [Note-3.3](#)).

The CERES instrument has an operational scanning cycle of 6.6 seconds and various scan elevation profiles. Radiometric measurements are sampled from the detectors every 0.01 seconds in all scanning profiles. The instrument makes Earth-viewing science measurements while the detectors rotate in the vertical (elevation scan) plane, and while the instrument horizontal (azimuth scan) plane is either fixed or rotating. The instrument has built-in calibration sources for performing in-flight calibrations, and can also be calibrated by measuring solar radiances reflected by a solar diffuser plate into the instrument field of view. See the In-flight Measurement Analysis document, DRL 64, provided by the CERES instrument builder TRW (Reference 3), and the CERES ATBD for Subsystem 1.0 (Reference 4).

4.0 Data Description

4.1 Spatial Characteristics

4.1.1 Spatial Coverage

The CERES collection is a global data set whose spatial coverage depends on the satellite orbit. The spatial coverage of the data contained on the ES-8 is shown in [Table 4-1](#).

Table 4-1. ES-8 Spatial Coverage

Spacecraft	Instrument	Minimum Latitude (deg)	Maximum Latitude (deg)	Minimum Longitude (deg)	Maximum Longitude (deg)	Spacecraft Altitude (km)
TRMM	PFM	-45	45	-180	180	350
Terra	FM1 & FM2	-90	90	-180	180	705
Aqua	FM3 & FM4	-90	90	-180	180	705

4.1.2 Spatial Resolution

The ES-8 contains measurement level data as described in this document's [Summary](#). The CERES FOV for a nadir viewing measurement is 10 km for TRMM and 20 km for both Terra and Aqua.

4.2 Temporal Characteristics

4.2.1 Temporal Coverage

CERES temporal coverage begins at different times depending upon when the spacecraft is launched, when the scan covers are opened after launch, and when early in-orbit calibration check-out is completed (see [Table 4-2](#)). The ES-8 contains 24 hours of data beginning at midnight GMT.

Table 4-2. CERES Temporal Coverage

Spacecraft	Instrument	Launch Date	Start Date	End Date
TRMM	PFM	11/27/1997	12/27/1997	8/31/1998a
Terra	FM1 & FM2	12/18/1999	02/24/2000	TBD
Aqua	FM3 & FM4	05/05/2002	06/19/2002	TBD

- a. The CERES instrument on TRMM has operated only occasionally since 9/1/98 due to a power converter anomaly.

4.2.2 Temporal Resolution

The ES-8 contains measurement level data as explained in this document's [Summary](#). These measurements are organized on the ES-8 according to 3.3-second scans in 6.6-second records. Each record contains 660 measurements. The measurement frequency is one per 0.01 seconds. [Table 4-3](#) shows the orbit inclination, altitude, and approximate number of Earth viewing measurements per record for each CERES spacecraft.

Table 4-3. CERES Orbit Characteristics

Spacecraft	Inclination	Altitude	Number of Earth-viewing Measurements
TRMM	35°	350 km	500
Terra	Sun-synchronous 10:30 a.m. Polar	705 km	390
Aqua	Sun-synchronous 1:30 p.m. Polar	705 km	390

4.3 Parameter Definitions

The ES-8 data product has been documented with several different elements. Acronyms and Units are explained in [Section 16.0](#). Some acronyms are linked to glossary “Terms” in [Section 15.0](#) which expand the description to a paragraph length. The formal definitions of the ES-8 parameters are in [Section 4.3](#) and begin with a short statement of the parameter followed by the units, range, and a link to a table which gives data type and dimension information. Following the short definition is a more complete definition, which may include additional information of less interest to some. When necessary, “Notes” in [Section 8.0](#) are given to expand on subjects that will help in the use and understanding of the ES-8 product. Notes are generally characterized by more details and longer length.

4.3.1 ES-8 V data

ES8-V1 Time at observation

The Julian Date (See [Term-10](#)) at scan sample 1 (See [Term-18](#)). (day) [2440000 .. 2480000] (See [Table 5-4](#))

The time of observation for any scan sample (See [Term-18](#)) is

$$t_n = t_1 + (n - 1) \left(\frac{0.01 \text{ sec}}{24 \times 60 \times 60 \text{ sec day}^{-1}} \right)$$

where t_1 =([ES8-V1](#)) and n=scan sample number from 1 to 660.

In Subsystem 1, the toolkit call PGS_TD_SCTime_to.UTC converts Spacecraft time to UTC time. A second toolkit call, PGS_TD_UTCToUTCjd, converts the ASCII string into two double precision real numbers, the Julian Date at Greenwich midnight and the fraction of the day since Greenwich midnight, which are added together to obtain the time of observation.

ES8-V2 Earth-Sun distance at record start

The distance from the Earth to the Sun in AU at the scan sample 1 (See [Term-18](#)). (AU) [0.98 .. 1.02] (See [Table 5-4](#))

In Subsystem 1, the toolkit call PGS_CBP_CB_Vector computes the Earth-Centered Inertial frame vector to the Sun. The toolkit call PGS_CSC_ECIttoECR transforms the position vector to the ECR or Earth equator, Greenwich meridian system (See [Term-3](#)). The magnitude of the position vector is then computed and converted from meters to AU.

ES8-V3 X component of satellite position at record start

The X component of the satellite position at scan sample 1 (See [Term-18](#)) in the Earth equator, Greenwich meridian system (See [Term-3](#)). (m) [-8×10^6 .. 8×10^6] (See [Table 5-4](#))

In Subsystem 1, the toolkit call PGS_EPH_Earth_EphemAttit computes the satellite position and velocity vector in Earth-Centered Inertial coordinates. A second toolkit call, PGS_CSC_ECIttoECR, transforms the position and velocity vector to the ECR or Earth equator, Greenwich meridian system (See [Term-3](#)).

ES8-V4 X component of satellite position at record end

The X component of the satellite position at scan sample 660 (See [Term-18](#)) in the Earth equator, Greenwich meridian system (See [Term-3](#)). (m) [-8×10^6 .. 8×10^6] (See [Table 5-4](#))

The satellite position components are determined from toolkit calls (See [ES8-V3](#)).

ES8-V5 Y component of satellite position at record start

The Y component of the satellite position at scan sample 1 (See [Term-18](#)) in the Earth equator, Greenwich meridian system (See [Term-3](#)). (m) [-8×10^6 .. 8×10^6] (See [Table 5-4](#))

The satellite position components are determined from toolkit calls (See [ES8-V3](#)).

ES8-V6 Y component of satellite position at record end

The Y component of the satellite position at scan sample 660 (See [Term-18](#)) in the Earth equator, Greenwich meridian system (See [Term-3](#)). (m) [-8×10^6 .. 8×10^6] (See [Table 5-4](#))

The satellite position components are determined from toolkit calls (See [ES8-V3](#)).

ES8-V7 Z component of satellite position at record start

The Z component of the satellite position at scan sample 1 (See [Term-18](#)) in the Earth equator, Greenwich meridian system (See [Term-3](#)). (m) $[-8 \times 10^6 .. 8 \times 10^6]$ (See [Table 5-4](#))

The satellite position components are determined from toolkit calls (See [ES8-V3](#)).

ES8-V8 Z component of satellite position at record end

The Z component of the satellite position at scan sample 660 (See [Term-18](#)) in the Earth equator, Greenwich meridian system (See [Term-3](#)). (m) $[-8 \times 10^6 .. 8 \times 10^6]$ (See [Table 5-4](#))

The satellite position components are determined from toolkit calls (See [ES8-V3](#)).

ES8-V9 X component of satellite velocity at record start

The X component of the satellite inertial velocity at scan sample 1 (See [Term-18](#)) in the Earth equator, Greenwich meridian system (See [Term-3](#)). (m sec⁻¹) $[-1 \times 10^4 .. 1 \times 10^4]$ (See [Table 5-4](#))

The satellite velocity components are determined from toolkit calls (See [ES8-V3](#)).

ES8-V10 X component of satellite velocity at record end

The X component of the satellite inertial velocity at scan sample 660 (See [Term-18](#)) in the Earth equator, Greenwich meridian system (See [Term-3](#)). (m sec⁻¹) $[-1 \times 10^4 .. 1 \times 10^4]$ (See [Table 5-4](#))

The satellite velocity components are determined from toolkit calls (See [ES8-V3](#)).

ES8-V11 Y component of satellite velocity at record start

The Y component of the satellite inertial velocity at scan sample 1 (See [Term-18](#)) in the Earth equator, Greenwich meridian system (See [Term-3](#)). (m sec⁻¹) $[-1 \times 10^4 .. 1 \times 10^4]$ (See [Table 5-4](#))

The satellite velocity components are determined from toolkit calls (See [ES8-V3](#)).

ES8-V12 Y component of satellite velocity at record end

The Y component of the satellite inertial velocity at scan sample 660 (See [Term-18](#)) in the Earth equator, Greenwich meridian system (See [Term-3](#)). (m sec⁻¹) $[-1 \times 10^4 .. 1 \times 10^4]$ (See [Table 5-4](#))

The satellite velocity components are determined from toolkit calls (See [ES8-V3](#)).

ES8-V13 Z component of satellite velocity at record start

The Z component of the satellite inertial velocity at scan sample 1 (See [Term-18](#)) in the Earth equator, Greenwich meridian system (See [Term-3](#)). (m sec⁻¹) $[-1 \times 10^4 .. 1 \times 10^4]$ (See [Table 5-4](#))

The satellite velocity components are determined from toolkit calls (See [ES8-V3](#)).

ES8-V14 Z component of satellite velocity at record end

The Z component of the satellite inertial velocity at scan sample 660 (See [Term-18](#)) in the Earth equator, Greenwich meridian system (See [Term-3](#)). (m sec^{-1}) [$-1 \times 10^4 \dots 1 \times 10^4$] (See [Table 5-4](#))

The satellite velocity components are determined from toolkit calls (See [ES8-V3](#)).

ES8-V15 Colatitude of satellite nadir at record start

The geocentric colatitude angle Θ (See [Figure 4-1](#)) of the satellite nadir point (See [Term-11](#)) at scan sample 1 (See [Term-18](#)) in the Earth equator, Greenwich meridian system (See [Term-3](#)). (deg) [0 .. 180] (See [Table 5-4](#))

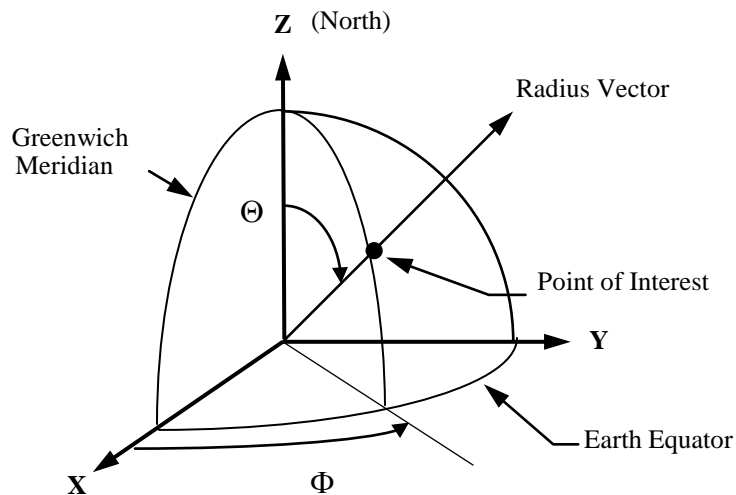


Figure 4-1. Colatitude and Longitude

The geocentric colatitude of nadir is the angle between the vector from the center of the Earth to the satellite and a vector normal to the Earth equator toward the North pole as defined in the Earth equator, Greenwich meridian system (See [Term-3](#)). An alternate formulation is given in [Note-2](#).

In Subsystem 1, the toolkit call PGS_EPH_EphemAttit computes the satellite position vector in Earth-Centered Inertial coordinates. A second toolkit call, PGS_CSC_ECIttoECR, transforms the position vector to the ECR or Earth equator, Greenwich meridian rectangular coordinate system and from this, the geocentric colatitude and longitude are calculated.

ES8-V16 Colatitude of satellite nadir at record end

The geocentric colatitude angle Θ (See [Figure 4-1](#)) of the satellite nadir point (See [Term-11](#)) at scan sample 660 (See [Term-18](#)) in the Earth equator, Greenwich meridian system (See [Term-3](#)). (deg) [0 .. 180] (See [Table 5-4](#))

The geocentric colatitude of nadir is the angle between the vector from the center of the Earth to the satellite and a vector normal to the Earth equator toward the North pole as defined in the Earth equator, Greenwich meridian system (See [Term-3](#)). An alternate formulation is given in [Note-2](#).

ES8-V17 Longitude of satellite nadir at record start

The longitude angle Φ (See [Figure 4-1](#)) of the satellite nadir point (See [Term-11](#)) at scan sample 1 (See [Term-18](#)) in the Earth equator, Greenwich meridian system (See [Term-3](#)). (deg) [0 .. 360] (See [Table 5-4](#))

The longitude of nadir is the angle in the Earth equator plane from the Greenwich meridian (See [Term-3](#)) to the nadir point meridian, rotating East. An alternate formulation is given in [Note-2](#).

ES8-V18 Longitude of satellite nadir at record end

The longitude angle Φ (See [Figure 4-1](#)) of the satellite nadir point (See [Term-11](#)) at scan sample 660 (See [Term-18](#)) in the Earth equator, Greenwich meridian system (See [Term-3](#)). (deg) [0 .. 360] (See [Table 5-4](#))

The longitude of nadir is the angle in the Earth equator plane from the Greenwich meridian (See [Term-3](#)) to the nadir point meridian, rotating East. An alternate formulation is given in [Note-2](#).

ES8-V19 Colatitude of Sun at observation

The geocentric colatitude angle of the Sun at scan sample 1 (See [Term-18](#)) in the Earth equator, Greenwich meridian system (See [Term-3](#)). (deg) [0 .. 180] (See [Table 5-4](#))

The geocentric colatitude of the Sun is the angle between the vector from the center of the Earth to the Sun and a vector normal to the Earth equator toward the North pole as defined in the Earth equator, Greenwich meridian system (See [Term-3](#)).

In Subsystem 1, the toolkit call PGS_CBP_Earth_CB_vector computes the sun position vector in Earth-Centered Inertial coordinates. A second toolkit call, PGS_CSC_ECIttoECR, transforms the position vector to the ECR or Earth equator, Greenwich meridian rectangular coordinate system and from this, the geocentric colatitude and longitude are calculated.

ES8-V20 Longitude of Sun at observation

The longitude angle of the Sun at scan sample 1 (See [Term-18](#)) in the Earth equator, Greenwich meridian system (See [Term-3](#)). (deg) [0 .. 360] (See [Table 5-4](#))

The longitude of the Sun is the angle in the Earth equator plane from the Greenwich meridian (See [Term-3](#)) to the Sun meridian, rotating East.

ES8-V21 Spectral Response Functions

The spectral response functions are spectral response values (unitless) [0 .. 1] at given wavelengths (microns) for the shortwave, total, and window channels used to create the spectral correction coefficients (See [Term-20](#)).

Spectral response function represent the spectral throughput of the detector optical component elements. The spectral response functions are used to spectrally correct the measured radiances that are passed through the optical path of each individual detector to obtain the unfiltered radiances dependent on the scene type (See [ES8-14](#)).

4.3.2 ES-8 Scientific Data Definitions

ES8-1 Colatitude of CERES FOV at TOA

This parameter is the geocentric colatitude angle Θ (See [Figure 4-1](#)) of the TOA point (See [Term-23](#)). (deg) [0 .. 180] (See [Table 5-3](#))

The geocentric colatitude of the TOA point is the angle between the vector from the center of the Earth to the TOA point (See [Term-23](#)) and a vector normal to the Earth equator toward the North pole as defined in the Earth equator, Greenwich meridian system (See [Term-3](#)).

If any part of the FOV is off the Earth “surface” (See [Term-4](#)), the FOV flag (See [ES8-18](#)) is set to bad and the colatitude is set to default. There are 660 values of this parameter per record; one for each measurement point (See [Term-17](#)).

In Subsystem 1, the toolkit call PGS_CSC_GetFOV_Pixel returns the geodetic latitude and longitude of the intersection of the FOV centroid and the CERES_TOA model. Another toolkit call PGS_CSC_GEOtoECR transforms the geodetic latitude and longitude to the ECR or Earth equator, Greenwich meridian rectangular coordinates from which the geocentric colatitude and longitude are calculated.

ES8-2 Longitude of CERES FOV at TOA

This parameter is the longitude angle Φ (See [Figure 4-1](#)) of the TOA point (See [Term-23](#)). (deg) [0 .. 360] (See [Table 5-3](#))

The longitude of the TOA point is the angle in the Earth equator plane from the Greenwich meridian (See [Term-3](#)) to the TOA point meridian, rotating East.

If any part of the FOV is off the Earth “surface” (See [Term-4](#)), the FOV flag (See [ES8-18](#)) is set to bad and the longitude is set to default. There are 660 values of this parameter per record; one for each measurement (See [Term-17](#)).

The longitude of the TOA point is determined from toolkit calls (See [ES8-1](#)).

ES8-3 CERES TOT filtered radiance

This parameter is the measured, spectrally integrated radiance emerging from the TOA, where the spectral integration is weighted by the spectral throughput of the TOT channel. It is the “raw” measurement from the TOT channel after count conversion (See [Term-2](#)) and is spectrally corrected (See [Term-20](#)) to yield the unfiltered LW radiance (See [ES8-10](#)) at night. The TOT and SW filtered radiances are spectrally corrected together to yield the LW radiance during the day. ($\text{W m}^{-2} \text{sr}^{-1}$) [-2 .. 700] (See [Table 5-3](#))

The value of the filtered TOT radiance is defined as either “good” or “bad” by the quality flag (See [ES8-15](#)). If the value is “bad,” for any reason, the TOT filtered radiance is set to a default value (See Section 4.4). If the value is “good,” the measured value is retained. There are 660 values of TOT filtered radiance per record; one for each measurement point (See [Term-17](#)).

The TOT filtered radiance is a measure of all radiance that passes through the TOT channel. The spectral weighting produced by the TOT channel throughput is the product of the primary mirror reflectance, the secondary mirror reflectance, and the absorptance of the detector flake. The TOT spectral throughput passes about 90% of the radiant power with wavelengths longer than 5 μm and about 85% of the power with shorter wavelengths.

ES8-4 CERES SW filtered radiance

This parameter is the measured, spectrally integrated radiance emerging from the TOA, where the spectral integration is weighted by the spectral throughput of the SW channel. It is the “raw” measurement from the SW channel after count conversion (See [Term-2](#)) and is spectrally corrected (See [Term-20](#)) to yield the unfiltered SW radiance (See [ES8-9](#)). ($\text{W m}^{-2} \text{sr}^{-1}$) [-4 .. 510] (See [Table 5-3](#))

The value of the SW filtered radiance is defined as either “good” or “bad” by the quality flag (See [ES8-16](#)). If the value is “bad,” for any reason, the SW filtered radiance is set to a default value (See Section 4.4). If the value is “good” the measured value is retained. There are 660 values of SW filtered radiance per record; one for each measurement point (See [Term-17](#)).

The SW filtered radiance is a measure of all radiance that passes through the SW channel. The spectral weighting produced by the SW channel throughput is the product of the SW filter throughput and the TOT channel throughput (See [ES8-3](#)). The SW spectral throughput passes about 75% of the radiant power with wavelengths shorter than 5 μm and cuts off rather sharply at about 5 μm . Wavelengths longer than this wavelength contribute a very small fraction of this measurement.

ES8-5 CERES WN filtered radiance

This parameter is a measured, spectrally integrated radiance emerging from the TOA, where the spectral integration is weighted by the spectral throughput of the WN channel. It has a bandpass from approximately 8 to 12 μm . It is the “raw” measurement from the window channel after count conversion (See [Term-2](#)) and is spectrally corrected (See [Term-20](#)) to yield the unfiltered WN radiance (See [ES8-11](#)). ($\text{W m}^{-2} \text{sr}^{-1} \mu\text{m}^{-1}$) [-1 .. 15] (See [Table 5-3](#))

The value of the WN filtered radiance is defined as either “good” or “bad” by the quality flag (See [ES8-17](#)). If the value is “bad,” for any reason, the WN filtered radiance is set to a default value (See Section 4.4). If the value is “good,” the measured value is retained. There are 660 values of WN filtered radiance per record; one for each measurement point (See [Term-17](#)).

The WN filtered radiance is a measure of all radiance that passes through the WN channel. The spectral weighting produced by the WN channel throughput is the product of the WN filter throughput and the TOT channel throughput (See [ES8-3](#)). The WN spectral throughput passes about 67% of the radiant power between 8 to 12 μm .

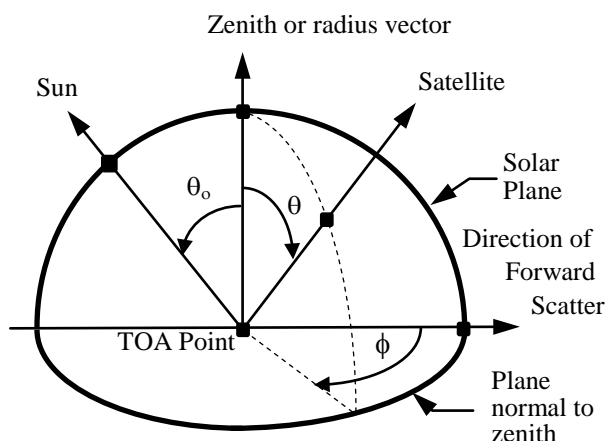
ES8-6 CERES viewing zenith at TOA

Figure 4-2. Viewing Angles at TOA

This parameter is the zenith angle θ (See Figure 4-2) at the TOA point (See Term-23) of the satellite. (deg)[0 .. 90] (See Table 5-3).

The viewing zenith is the angle between the radius vector from the center of the Earth to the TOA point and a vector from the TOA point to the satellite. There are 660 values of viewing zenith per record; one for each measurement point (See Term-17).

ES8-7 CERES solar zenith at TOA

This parameter is the zenith angle θ_o (See Figure 4-2) at the TOA point (See Term-23) of the Sun. (deg) [0 .. 180] (See Table 5-3)

The solar zenith is the angle between the radius vector from the center of the Earth to the TOA point and a vector from the TOA point to the Sun. There are 660 values of solar zenith per record; one for each measurement point (See Term-17).

ES8-8 CERES relative azimuth at TOA

This parameter is the azimuth angle ϕ (See Figure 4-2) at the TOA point (See Term-23) of the satellite relative to the solar plane. (deg) [0 .. 360] (See Table 5-3)

The relative azimuth is measured clockwise in the plane normal to the zenith so that the relative azimuth of the Sun is always 180° . The solar plane is the plane which contains the radius vector (zenith) and a vector from the TOA point to the Sun. If the TOA point is north of the subsolar point (See Term-21) on the same meridian, then an azimuth of 90° would imply the satellite is east of the TOA point. There are 660 values of relative azimuth per record; one for each measurement point (See Term-17).

ES8-9 CERES SW unfiltered radiance

This parameter is an estimate of the solar radiance at all wavelengths reflected back into space and contains no thermal radiance. ($\text{W m}^{-2} \text{sr}^{-1}$) [-10 .. 510] (See [Table 5-3](#))

It is a spectrally integrated radiance that is intended to represent the radiance of reflected sunlight. In other words, the SW unfiltered radiance is the radiance we would observe if we had a spectrally flat channel that passed all the reflected sunlight and that removed any thermal emission from the Earth and the Earth's atmosphere. Frequently, in informal discussion, we incorrectly refer to the SW unfiltered radiance as a broadband radiance covering the spectral interval from 0 to 5 μm .

At night the SW radiance is set to zero where night is defined as a solar zenith angle ([ES8-7](#)) greater than 90° at the TOA point (See [Term-23](#)). During the day, the SW radiance, I^{SW} , is defined by $I^{\text{SW}} = C^{\text{SW}}(m_f^{\text{SW}} - \text{SW}^{\text{offset}})$ where C^{SW} is from a set of spectral correction coefficients (See [Term-20](#)), m_f^{SW} is the filtered shortwave measurement ([ES8-4](#)), and $\text{SW}^{\text{offset}}$ is an estimate of the thermal radiance measured by the shortwave channel and is either zero or the average nighttime shortwave measurement for the previous nighttime passage. $\text{SW}^{\text{offset}}$ is updated each satellite revolution or as often as 15 times for a 24-hour period.

There are 660 values of the SW unfiltered radiance per record; one for each measurement point (See [Term-17](#)).

The unfiltered SW radiance is “good” if it contains a non-default value. If the filtered SW radiance is flagged “bad” (See [ES8-16](#)), then the unfiltered SW radiance is set to default (See [Section 4.4](#)). If the FOV Flag is “bad” (See [ES8-18](#)), or the SW ADM is greater than 2 (See [Note-4](#)), then the unfiltered SW radiance is set to default. No other condition will cause the SW unfiltered radiance on the ES-8 to be set to default.

ES8-10 CERES LW unfiltered radiance

This parameter is an estimate of the thermal radiance at all wavelengths emitted to space including shortwave thermal radiance and including no solar reflected radiance. ($\text{W m}^{-2} \text{sr}^{-1}$) [0 .. 200] (See [Table 5-3](#))

It is a spectrally integrated radiance that is intended to represent the radiance from emission of the atmosphere and the Earth that emerges from the top of the atmosphere. In other words, the LW unfiltered radiance is the radiance that we would observe if we had a spectrally flat channel that passed all the emitted radiance and that removed any reflected sunlight. Frequently, in informal discussion, we incorrectly refer to the LW unfiltered radiance as a broadband radiance covering wavelengths longer than 5 μm .

At night the LW radiance I^{LW} is defined by $I^{\text{LW}} = C^{\text{TOT}} m_f^{\text{TOT}}$ where C^{TOT} is from a set of spectral correction coefficients (See [Term-20](#)), m_f^{TOT} is the filtered total measurement (See [ES8-3](#)), and where night is defined as a solar zenith angle (See [ES8-7](#)) greater than 90° at the TOA point (See [Term-23](#)). During the day, the LW radiance is defined as the TOT radiance minus the SW radiance with the appropriate spectral correction coefficients, or by $I^{\text{LW}} = C^{\text{TOT}} m_f^{\text{TOT}} +$

$C^{SW} (m_f^{SW} - SW^{offset})$ where C^{TOT} and C^{SW} are from a set of spectral correction coefficients (See [Term-20](#)), m_f^{SW} is the filtered shortwave measurement (See [ES8-4](#)), and SW^{offset} is an estimate of the thermal radiation in the shortwave measurement (See [ES8-9](#)).

There are 660 values of the LW unfiltered radiance per record; one for each measurement point (See [Term-17](#)).

The unfiltered LW radiance is “good” if it contains a non-default value. If the filtered TOT radiance is flagged “bad” (See [ES8-15](#)), then the unfiltered LW radiance is set to default (See [Section 4.4](#)). During the day, the unfiltered LW radiance is set to default if the filtered SW radiance is flagged “bad.” If the FOV Flag is “bad” (See [ES8-18](#)), or the SW ADM is greater than 2 (See [Note-4](#)), then the unfiltered LW radiance is set to default. No other condition will cause the LW unfiltered radiance on the ES-8 to be set to default.

The spectral correction (See [Term-20](#)) which converts the filtered radiance to unfiltered radiance is dependent on the scene type (See [ES8-14](#)). If the SW ADM is greater than 2, then the scene identified by the MLE (See [Note-5](#)) is questionable and the spectral correction is not performed. This will result in default values for both the unfiltered radiance and flux (See [ES8-13](#)).

ES8-11 CERES WN unfiltered radiance

This parameter is an estimate of the average radiance per micrometer in the spectral window from 8.0 to 12.0 microns. This radiance is dominated by emission from the Earth's surface when the scene is clear. ($W m^{-2} sr^{-1} \mu m^{-1}$) [0 .. 15] (See [Table 5-3](#))

The unfiltered WN radiance is defined by $I^{WN} = C^{WN} m_f^{WN}$ where C^{WN} is from a set of spectral correction coefficients (See [Term-20](#)), and m_f^{WN} is the filtered window measurement (See [ES8-5](#)). There are 660 values of the WN unfiltered radiance per record; one for each measurement point (See [Term-17](#)).

The unfiltered WN radiance is “good” if it contains a non-default value. If the filtered WN radiance is flagged “bad” (See [ES8-17](#)), then the unfiltered WN radiance is set to default (See [Section 4.4](#)). If the FOV Flag is “bad” (See [ES8-18](#)), or the SW ADM is greater than 2 (See [Note-4](#)), then the unfiltered WN radiance is set to default. No other condition will cause the WN unfiltered radiance on the ES-8 to be set to default.

The spectral correction (See [Term-20](#)) which converts the filtered radiance to unfiltered radiance is dependent on the scene type (See [ES8-14](#)). If the SW ADM is greater than 2, then the scene identified by the MLE (See [Note-5](#)) is questionable and the spectral correction is not performed. This will result in a default value for the WN unfiltered radiance.

ES8-12 CERES SW flux at TOA

This parameter is an estimate of the solar flux at all wavelengths reflected back into space at the TOA point (See [Term-23](#)). ($W m^{-2}$) [0 .. 1400] (See [Table 5-3](#))

At night the SW flux is set to zero where night is defined as a solar zenith angle (See [ES8-7](#)) greater than 90° at the TOA point (See [Term-23](#)). The SW flux is set to default (See [Section 4.4](#)) when the solar zenith angle is between 86.5° and 90.0° . When the solar zenith is less than or equal to 86.5° , the SW flux \hat{M}^{SW} is given by

$$\hat{M}^{SW} = \frac{\pi I^{SW}}{R^i(\theta, \phi, \theta_o)}$$

where I^{SW} is the shortwave radiance (See [ES8-9](#)), and R is the anisotropy (or [ADM](#), See [Note-4](#)) for the i^{th} scene type (See [ES8-14](#)); and R is evaluated at the viewing zenith angle θ (See [ES8-6](#)), relative azimuth angle ϕ (See [ES8-8](#)), and solar zenith angle θ_o (See [ES8-7](#)).

There are 660 values of the SW flux per record; one for each measurement point (See [Term-17](#)).

The SW flux is set to default if the SW radiance (See [ES8-9](#)) is default, or if the scene type (See [ES8-14](#)) is unknown, or if the instrument is operating in the rapid retrace mode ([ES8-19](#)).

During the day, $albedo = \hat{M}^{SW} / (E \cos \theta_o)$ where $E=1365 \text{ d}^{-2}$ and $d=(\text{ES8-V2})$. If albedo is greater than 1.0 or less than 0.02, the SW flux is set to default. The SW flux is also set to default for geometric conditions that lead to inaccurate flux estimates, or for $\theta > 70^\circ$, $86.5^\circ < \theta_o \leq 90^\circ$, and $R^i \geq 2$.

ES8-13 CERES LW flux at TOA

This parameter is an estimate of the thermal flux at all wavelengths emitted to space at the TOA point (See [Term-23](#)) including shortwave thermal flux. (W m^{-2}) [50 .. 450] (See [Table 5-3](#))

The LW flux \hat{M}^{LW} is given by

$$\hat{M}^{LW} = \frac{\pi I^{LW}}{R^i(\theta, \Theta)}$$

where I^{LW} is the longwave radiance (See [ES8-10](#)), and R is the anisotropy (or [ADM](#), See [Note-4](#)) for the i^{th} scene type (See [ES8-14](#)); and R is evaluated at the viewing zenith angle θ (See [ES8-6](#)), and colatitude of the TOA point Θ (See [ES8-1](#)).

There are 660 values of the LW flux per record; one for each measurement point (See [Term-17](#)).

The LW flux is set to default (See [Section 4.4](#)) if the LW radiance (See [ES8-10](#)) is default, or if the scene type (See [ES8-14](#)) is unknown, or if the instrument is operating in the rapid retrace mode (See [ES8-19](#)), or if the flux is greater than 400 W m^{-2} or less than 50 W m^{-2} . The LW flux is also set to default for geometric conditions that lead to inaccurate flux estimates, or for $\theta > 70^\circ$.

ES8-14 ERBE scene identification at observation

This parameter is an estimate of the scene at the TOA point as determined by the MLE scene identification algorithm (See [Note-5](#)). (N/A) [0 .. 12.4] (See [Table 5-3](#))

The 13 possible ERBE scene types are listed in [Table 4-4](#).

Table 4-4. ERBE Scene Types

ES8-14 VALUE	DESCRIPTION OF SCENE	Cloud Cover
0.X	unknown scene	
1.X	clear ocean	0 - 5 %
2.X	clear land	0 - 5 %
3.X	clear snow	0 - 5 %
4.X	clear desert	0 - 5 %
5.X	clear land-ocean mix	0 - 5 %
6.X	partly cloudy over ocean	5 - 50 %
7.X	partly cloudy over land or desert	5 - 50 %
8.X	partly cloudy over land-ocean mix	5 - 50 %
9.X	mostly cloudy over ocean	50 - 95 %
10.X	mostly cloudy over land or desert	50 - 95 %
11.X	mostly cloudy over land-ocean mix	50 - 95 %
12.X	overcast	95 - 100 %

where a land-ocean mix scene denotes 50% land and 50% ocean and is used for coastal areas and where X equals 0, 1, 2, 3, 4 for ocean, land, snow, desert, land-ocean mix, respectively. The decimal defines the geographic scene so that 12.1 would indicate overcast over land, etc. Care should be taken in determining the geographic scene from the decimal because of computer characteristics. A useful Fortran code is

$$\text{ISCENE} = \text{NINT}(\text{ES8-14})$$

$$\text{IX} = \text{NINT}(((\text{ES8-14}) - \text{REAL}(\text{ISCENE})) * 10.0)$$

where NINT is the nearest integer operator and IX is the geographic scene index.

There are 660 values of the ERBE scene per record; one for each measurement point (See [Term-17](#)).

ES8-15 TOT channel flag words

This parameter contains twenty two 32-bit words where a single bit defines the quality of the filtered TOT radiance (See [ES8-3](#)) as “good” (bit=0) or “bad” (bit=1). There are 660 bit flags per record; one for each measurement point (See [Term-17](#)). (N/A) [N/A] (See [Table 5-3](#))

The ordering of the bit flags is given in [Table 4-5](#) where bit 32 is the “sign” bit and bit 31 is extra so that we have 22 words \times 30 bits = 660 bit flags.

Table 4-5. Bit Order for Radiometric and FOV Quality Flags

Word	Bit Order								
	32 a	31 b	30	29	28	27 ... 4	3	2	1
1			30	29	28		3	2	1
2			60	59	58		33	32	31
3			90	89	88		63	62	61
20			600	599	598		573	572	571
21			630	629	628		603	602	601
22			660	659	658		633	632	631

- a. Sign Bit
- b. Extra Bit

ES8-16 SW channel flag words

This parameter contains twenty two 32-bit words where a single bit defines the quality of the filtered SW radiance (See [ES8-4](#)) as “good” (bit=0) or “bad” (bit=1). There are 660 bit flags per record; one for each measurement point (See [Term-17](#)). (N/A) [N/A] (See [Table 5-3](#))

The ordering of the bit flags is given in [Table 4-5](#) where bit 32 is the “sign” bit and bit 31 is extra so that we have 22 words \times 30 bits = 660 bit flags.

ES8-17 WN channel flag words

This parameter contains twenty two 32-bit words where a single bit defines the quality of the filtered WN radiance (See [ES8-5](#)) as “good” (bit=0) or “bad” (bit=1). There are 660 bit flags per record; one for each measurement point (See [Term-17](#)). (N/A) [N/A] (See [Table 5-3](#))

The ordering of the bit flags is given in [Table 4-5](#) where bit 32 is the “sign” bit and bit 31 is extra so that we have 22 words \times 30 bits = 660 bit flags.

ES8-18 Scanner FOV flag words

This parameter contains twenty two 32-bit words where a single bit defines the quality of the FOV as “good” (bit=0) or “bad” (bit=1). A good FOV falls entirely on the surface (not TOA) of the Earth (See [Term-6](#)). All other FOVs are flagged bad. There are 660 bit flags per record; one for each measurement point (See [Term-17](#)). (N/A) [N/A] (See [Table 5-3](#))

The ordering of the bit flags is given in [Table 4-5](#) where bit 32 is the “sign” bit and bit 31 is extra so that we have 22 words \times 30 bits = 660 bit flags.

ES8-19 Rapid retrace flag words

This parameter contains twenty two 32-bit words where a single bit defines the state of the scan rate as “not in rapid retrace” (bit=0) or “in rapid retrace” (bit=1). Rapid retrace (See [Term-13](#)) occurs during the short scan mode (See [ES8-20](#)). There are 660 rapid retrace bit flags per record; one for each measurement point (See [Term-17](#)). (N/A) [N/A] (See [Table 5-3](#))

The ordering of the bit flags is given in [Table 4-5](#) where bit 32 is the “sign” bit and bit 31 is extra so that we have 22 words \times 30 bits = 660 bit flags.

ES8-20 Scanner operations flag word

This parameter contains three 32-bit words which define the scanner operations during the 6.6-sec record. The individual bits are defined in [Table 4-6](#), [Table 4-7](#), and [Table 4-8](#). Additional details follow the tables. (N/A) [N/A] (See [Table 5-3](#))

Table 4-6. Scanner Operations Flag Word 1 (of 3)

Bit Position (Right to Left)	Bit Value	Detail Description	Meaning
0-3	0000 0001 0010 0011 0100 0101 0110 0111 1000 1001 1010 1011 1100-1111	ES8-20-A	<u>The Instrument is in the following Mode:</u> Safe Mode Standby Mode Crosstrack Mode Biaxial Mode Solar Calibration Mode Diagnostic Configuration Mode Internal Calibration Mode Special Short Scan Mode Contamination Safe Mode Hold Mode Abbreviated Internal Calibration Mode Fixed Azimuth Mode Undefined
4-5	00 01 10,11		Elevation Motor Drive Enabled Elevation Motor Drive Disabled Undefined
6-7	00 01 10,11		Azimuth Motor Drive Enabled Azimuth Motor Drive Disabled Undefined

Table 4-6. Scanner Operations Flag Word 1 (of 3)

Bit Position (Right to Left)	Bit Value	Detail Description	Meaning
8-9	00		Instrument Previous Mode (See bit 0-3) not in Solar Calibration or Internal Calibration
	01		Instrument Previous Mode in Solar Calibration
	10		Instrument Previous Mode in Internal Calibration
	11		Undefined
10-11	00		Instrument not in Internal Calibration
	01		Instrument in Internal Calibration
	10,11		Undefined
12-14	000		SWICS Lamp off
	001		SWICS Intensity at Level 1
	010		SWICS Intensity at Level 2
	011		SWICS Intensity at Level 3
	100-111		Undefined
15-30			Spares
31	0		At least one scanner radiometric value (ES8-3 - ES8-5) has both a good radiometric flag (ES8-15 - ES8-17) and a good FOV flag (ES8-18)
	1		If the above situation does not exist, record will not be included on the ES-8 product.

See detail descriptions after [Table 4-8](#).

Table 4-7. Scanner Operations Flag Word 2 (of 3)

Bit Position (Right to Left)	Bit Value	Detail Description	Meaning
0-4	00000 00001 00010 00011 00100 00101 00110 00111 01000 01001 01010 01011 01100 01101 01110 01111 10000-11111	ES8-20-B	The Scanner is in the following <u>Elevation Scan Profiles:</u> Stow Normal Earth Scan Short Earth Scan MAM Scan Nadir Scan Scan Profile 6 Scan Profile 7 Scan Profile 8 Scan Profile 9 Scan Profile 10 Scan Profile 11 Scan Profile 12 Scan Profile 13 Scan Profile 14 Scan Profile 15 Scan Profile 16 Undefined
5-8	0000 0001 0010 0011 0100 0101 0110 0111 1000 1001 1010 1011-1111	ES8-20-C	The last azimuth command is given below: Go To Position Crosstrack Go To Position A Go To Position B Go To Position Solar Calibration Go To Position Caged Go To Position Spare 1 Go To Position Spare 2 Go To Position Spare 3 Scan A B Asynchronously Scan A B Synchronously Stop Azimuth Undefined
9-11	000 001 010 011 100 101-111	ES8-20-D	Normal Scan Operation Initialization In Progress At Initialized Position Scan Abort In Progress Elevation At Aborted Position Undefined

Table 4-7. Scanner Operations Flag Word 2 (of 3)

Bit Position (Right to Left)	Bit Value	Detail Description	Meaning
12-14	000 001 010 011 100 101-111	ES8-20-E	Azimuth At Go To Position Azimuth At Stopped Position Azimuth At Initial Position Azimuth At Scan Position Azimuth In Motion Undefined
15	0 1		Instrument in Biaxial mode and azimuth is moving forward from 90° toward 270°. Instrument in Biaxial mode and azimuth is moving backward from 270° toward 90°.
16-31			Spares

See detail descriptions after [Table 4-8](#).

Table 4-8. Scanner Operations Flag Word 3 (of 3)

Bit Position (Right to Left)	Bit Value	Detail Description	Meaning
0-1	00 01 10 11	ES8-20-F	Instrument in FAPS Crosstrack (+/- 45°) Mode Instrument in RAPS Mode Instrument in FAPS Alongtrack (not crosstrack) Mode Instrument in Transitional Mode
2-31			Spares

ES8-20-A Instrument Mode:

Instrument in Safe Mode: The instrument is stowed during the safe mode for protection. If the solar presence sensors confirm the Sun is within the FOV of the sensors and that potential damage to the radiometers may result, the instrument will be automatically commanded to the Safe Mode.

Instrument in Standby Mode: The instrument is stowed during the Standby Mode.

Instrument in Crosstrack Mode: The azimuth is fixed to scan perpendicular to the satellite ground track. The elevation scan mode is either normal, short, or nadir scan (See [ES8-20-B](#)).

Instrument in Biaxial Mode: Both azimuth and elevation are operational. Azimuth rotation starts with the elevation scan plane in the along-track direction and rotates through 180 deg until the scan plane is again in the along-track direction,

the process is then reversed. Azimuth rotation is continuous at a rate up to 6 deg sec⁻¹.

Instrument in Solar Calibration Mode: The instrument is oriented in azimuth and elevation to view the MAM.

Instrument in Diagnostic Configuration Mode: The instrument must be in the diagnostic mode to accept the following commands: scan table loads, internal command sequence loads, and special diagnostic loads.

Instrument in Internal Calibration Mode: Internal calibration is invoked by commands which control the blackbody sources and the SWICS. The scan profile is the same as Normal Earth Scan (See [ES8-20-B](#)) (Crosstrack Mode or Biaxial Mode) except that the blackbody heater and SWICS lamp are powered on. During internal calibration the instrument total and longwave sensors view the on-board blackbodies for calibration. The shortwave sensor views the SWICS. Internal calibrations are performed approximately every two weeks in orbit.

Instrument in Special Short Scan Mode

Instrument in Contamination Safe Mode: This mode is intended to minimize the modification of time tagged commands stored on board the spacecraft in the event a velocity maneuver is planned after the 24 hour command upload for the instruments is completed. The instrument will be stowed, all calibration sources turned off, the azimuth will be rotated to a safe position, and the instrument will remain in this mode for 10 minutes and then automatically go to the Standby Mode.

Instrument in Hold Mode: Same as Standby Mode above.

Instrument in Abbreviated Internal Calibration Mode: This mode is similar to the Internal Calibration Mode with fewer sequences.

Instrument in Fixed Azimuth Mode: The azimuth is fixed at an angle (See [ES8-20-F](#)) to scan other than perpendicular to the satellite ground track (Crosstrack Mode). The exact azimuth angle is not included on the ES-8 product. The elevation scan profile is either Normal, Short, or Nadir Scan (See [ES8-20-B](#)).

ES8-20-B Elevation Scan Profiles:

Stow

Normal Earth Scan: The scan consists of scanning across the Earth. The sensor starts at space view, scans across the Earth, pauses at the opposite space look and slews up into the structure to view the (unpowered) internal calibration sources. The entire sequence is then reversed. The complete scan cycle is 6.6 sec in duration (See [Term-13](#)).

Short Earth Scan: The instrument goes into the short scan mode to protect the sensors from direct solar viewing if activated via ground command or the solar presence sensors. This mode is the same as the normal scan mode, except that the scan

terminates 16 deg in elevation below the earth limb and begins rapid retrace (See [Term-13](#)) prior to the earth limb to avoid direct solar viewing. This mode is required only in the Biaxial Mode.

The Short Earth Scan assumes the Sun will only appear on one side of the satellite. The Sun is kept on one side by carefully choosing azimuth scan turn around points which are usually 180 deg apart, but under some conditions, the turn around points will be “pinched” (less than 180 deg apart) to make sure that the Sun remains on the “sun” side of the instrument.

MAM Scan: This scan profile is used during the Instrument Solar Calibration Mode. A nominal MAM scan starts with the sensors viewing space for a zero reference. The sensors are then rotated in elevation to view the MAM. The sensors are rotated back to space for another space look. Next the sensors are rotated to view the instrument’s internal calibration sources (blackbody and SWICS) and finally back to view space again. This cycle repeats every 6.6 sec.

Nadir Scan: During the nadir scan mode the scan pauses at nadir and then retraces to space look. This mode is used primarily during ground test and calibration.

Scan Profile 6 through Scan Profile 16: These profiles are programmable and used for special purposes at selected times.

ES8-20-C Last Azimuth Command:

Go To Position Crosstrack: The azimuth is rotated to the crosstrack position (See [ES8-20-A](#)) so that the scan is perpendicular to the satellite groundtrack.

Go To Position A: The azimuth is rotated to position A which is the starting position of the Biaxial Mode. The azimuth A is nominally in the forward alongtrack position, but is programmable to any value. The exact value of A is not included on the ES-8 product.

Go To Position B: The azimuth is rotated to position B which is the ending position of the Biaxial Mode. The azimuth B is nominally in the backward alongtrack position, but is programmable to any value. The exact value of B is not included on the ES-8 product.

Go To Position Solar Calibration: The azimuth is rotated to the position to view the MAM.

Go To Position Caged: The azimuth is rotated to the caged position.

Go To Position Spare 1: The azimuth is rotated to the spare 1 input position.

Go To Position Spare 2: The azimuth is rotated to the spare 2 input position.

Go To Position Spare 3: The azimuth is rotated to the spare 3 input position.

Scan A B Asynchronously: The azimuth is rotated to position A which is the starting position of the Biaxial Mode. When the azimuth reaches position A it then rotates to position B. This process is repeated until commanded otherwise.

Scan A B Synchronously: This is similar to the Scan A B Asynchronously command except in this command the instrument will synchronize the beginning of the 6.6 sec elevation scan cycle and the azimuth rotation cycle. The instrument will adjust the pause at the end of each azimuth cycle (at both A and B position) so that the cycles are always synchronized.

Stop Azimuth: The azimuth scan rate is immediately set to zero and the azimuth position held.

ES8-20-D Scan Mode:

Normal Scan Operation

Initialization In Progress

At Initialized Position

Scan Abort In Progress

Elevation At Aborted Position

ES8-20-E Azimuth Position:

Azimuth At Go To Position

Azimuth At Stopped Position

Azimuth At Initial Position

Azimuth At Scan Position

Azimuth In Motion

ES8-20-F Azimuth Plane Position:

Instrument in FAPS Crosstrack ($\pm 45^\circ$) Mode: The azimuth is fixed at a value within 45 deg of the perpendicular to the satellite groundtrack.

Instrument in RAPS Mode: The instrument is in the Biaxial Mode.

Instrument in FAPS Alongtrack (not crosstrack) Mode: The azimuth is fixed at a value greater than 45 deg from the perpendicular to the satellite groundtrack.

Instrument in Transitional Mode: The azimuth is in transition between modes.

4.4 Fill Values

Table 4-9 lists the default CERES Fill Values. Individual parameter definitions in the previous section explain how and when the default values are used. The CERES default fill values used on the ES-8 are defined as follows:

Table 4-9. CERES Fill Values

Fill Value Name	Value	Fill Value Description*
INT4_DFLT	2147483647	default value for a 4-byte integer
REAL4_DFLT	3.4028235E+38	default value for a 4-byte real
REAL8_DFLT	1.7976931348623157E+308	default value for a 8-byte real

4.5 Sample Data File

A sample data granule (See [Term-9](#)) containing 5 ES-8 records is part of a package which also includes sample read software (in C), a Readme file, a postscript file describing granule contents, and an ASCII listing of the data in the sample granule (data dump). The sample ES-8 package can be ordered from the Langley ASDC (See Section [12.0](#)). It is available from the Langley ASDC Web Ordering Tool and has the name format: CERES_Test_ES8_version information.

5.0 Data Organization

[Table 5-1](#) gives an overview of the ES-8 product. The metadata structures contain information which need only be recorded once per daily product. The CERES Baseline Header Metadata and the CERES_metadata Vdata are listed in Appendix A. As explained in Appendix A, the CERES Baseline Header Metadata includes either the bounding rectangle or GRing attributes. The spatial boundaries of the ES-8 are defined with the bounding rectangle. The ES-8 also contains Product Specific Metadata, which are shown in [Table 5-2](#).

Table 5-1. ES-8 Product Summary

HDF Name	Description	Number of Parameters	Nominal Size (MB)
CERES Baseline Header Metadata	See Table A-1	36	
CERES_metadata Vdata	See Table A-2	14	
ES-8 Product Specific Metadata	See Table 5-2	1	
ES-8 Metadata Size (MB/Day)			0.880
ES-8 Vdata Summary	See Table 5-4	20	1.120
ES-8 SDS Summary	See Table 5-3	20	467.108
ES-8 Data Size (MB/Day)			468.228
ES-8 Total Product Size (MB/Day)			469.087
ES-8 Total Product Size with HDF Data Compression			293.5a

a. GZIP Compression, Level 1

Table 5-2. ES-8 Product Specific Metadata

Item	Parameter Name	Records	Units	Range	Data Type
1	ES8_ProductionDate	1	N/A	N/A	ASCII string
2	NumOfCrosstrackRecords	1	N/A	0 .. 13092	Integer
3	NumOfRAPSRRecords	1	N/A	0 .. 13092	Integer
4	NumOfAlongtrackRecords	1	N/A	0 .. 13092	Integer
5	NumOfTransitionalRecords	1	N/A	0 .. 13092	Integer
6	Software_SCCR_Number	1	N/A	N/A	ASCII string
7	Data_SCCR_Number	1	N/A	N/A	ASCII string

5.1 Data Granularity

All ES-8 HDF data granules consist of no more than 24 hours of data from one CERES instrument.

5.2 ES-8 HDF Scientific Data Sets (SDS)

The ES-8 contains 20 SDSs (See [Term-19](#)) which are 2-dimensional arrays of time ordered records where the first dimension corresponds to the number of data records contained in the data-day; the maximum is 13,092 (since the time length of a record may vary, the maximum number of records on the ES-8 can be 13,092). For the measurement-level data, other than flag words, the second dimension corresponds to the number of measurements or footprints contained on an individual data record (660). There are 22 measurement-level, 32-bit flag words that contain a flag value in each of the right-most 30 bits (22 words x 30 bits/word = 660 bits). For these measurement-level flag words, the second dimension is 22. See [ES8-15](#) in [4.3.2](#) for a detailed explanation of the measurement-level flag words. [Table 5-3](#) summarizes the content and size of each SDS contained within the ES-8 file. The Item identification given in the table for each parameter may be used to find the parameter descriptions in [4.3.2](#).

Table 5-3. ES-8 SDS Summary

Item	Parameter Name (SDS Name)	Units	Range	Maximum Number of SDS Elements	Data Type	Maximum SDS Size (MB)
ES8-1	Colatitude of CERES FOV at TOA	deg	0 .. 180	13092 : .660	32 bit real	32.962
ES8-2	Longitude of CERES FOV at TOA	deg	0 .. 360	13092 : .660	32 bit real	32.962
ES8-3	CERES TOT filtered radiance	$W m^{-2} sr^{-1}$	-2 .. 700	13092 : .660	32 bit real	32.962
ES8-4	CERES SW filtered radiance	$W m^{-2} sr^{-1}$	-4 .. 510	13092 : .660	32 bit real	32.962
ES8-5	CERES WN filtered radiance	$W m^{-2} sr^{-1} \mu m^{-1}$	-1 .. 15	13092 : .660	32 bit real	32.962
ES8-6	CERES viewing zenith at TOA	deg	0 .. 90	13092 : .660	32 bit real	32.962
ES8-7	CERES solar zenith at TOA	deg	0 .. 180	13092 : .660	32 bit real	32.962
ES8-8	CERES relative azimuth at TOA	deg	0 .. 360	13092 : .660	32 bit real	32.962
ES8-9	CERES SW unfiltered radiance	$W m^{-2} sr^{-1}$	-10 .. 510	13092 : .660	32 bit real	32.962
ES8-10	CERES LW unfiltered radiance	$W m^{-2} sr^{-1}$	0 .. 200	13092 : .660	32 bit real	32.962
ES8-11	CERES WN unfiltered radiance	$W m^{-2} sr^{-1} \mu m^{-1}$	0 .. 15	13092 : .660	32 bit real	32.962
ES8-12	CERES SW flux at TOA	$W m^{-2}$	0 .. 1400	13092 : .660	32 bit real	32.962
ES8-13	CERES LW flux at TOA	$W m^{-2}$	50 .. 450	13092 : .660	32 bit real	32.962
ES8-14	ERBE scene identification at observation	N/A	0 .. 12.4	13092 : .660	32 bit real	32.962
ES8-15	TOT channel flag words	N/A	N/A	13092 : .22	32 bit integer	1.099
ES8-16	SW channel flag words	N/A	N/A	13092 : .22	32 bit integer	1.099
ES8-17	WN channel flag words	N/A	N/A	13092 : .22	32 bit integer	1.099
ES8-18	Scanner FOV flag words	N/A	N/A	13092 : .22	32 bit integer	1.099
ES8-19	Rapid retrace flag words	N/A	N/A	13092 : .22	32 bit integer	1.099

Table 5-3. ES-8 SDS Summary

Item	Parameter Name (SDS Name)	Units	Range	Maximum Number of SDS Elements	Data Type	Maximum SDS Size (MB)
ES8-20	Scanner operations flag word	N/A	N/A	13092 :: 3	32 bit integer	0.150
Total SDS Size						467.11

5.3 ES-8 HDF Vertex Data (Vdata)

The ES-8 contains 20 record-level parameters written by HDF-EOS as HDF Vdata structures. These structures may be thought of as one-dimensional arrays dimensioned according to the number of data records contained in the data-day; the maximum is 13,092 (since the time length of a record may vary, the maximum number of records on the ES-8 can be 13,092). Each of these arrays contains one of the parameters listed in [Table 5-4](#). The Item identification given in the table for each parameter may be used to find the parameter descriptions in [4.3.1](#).

Table 5-4. ES-8 Vdata Summary

Item	Parameter Name (Vdata Name)	Units	Range	Maximum Number of Vdata Elements	Data Type	Maximum Vdata Size (MB)
ES8-V1	Time of observation	day	2440000 .. 2480000	13092	64 bit real	0.100
ES8-V2	Earth-Sun distance at record start	AU	0.98 .. 1.02	13092	64 bit real	0.100
ES8-V3	X component of satellite position at record start	m	$-8 \cdot 10^6$.. $8 \cdot 10^6$	13092	32 bit real	0.050
ES8-V4	X component of satellite position at record end	m	$-8 \cdot 10^6$.. $8 \cdot 10^6$	13092	32 bit real	0.050
ES8-V5	Y component of satellite position at record start	m	$-8 \cdot 10^6$.. $8 \cdot 10^6$	13092	32 bit real	0.050
ES8-V6	Y component of satellite position at record end	m	$-8 \cdot 10^6$.. $8 \cdot 10^6$	13092	32 bit real	0.050
ES8-V7	Z component of satellite position at record start	m	$-8 \cdot 10^6$.. $8 \cdot 10^6$	13092	32 bit real	0.050
ES8-V8	Z component of satellite position at record end	m	$-8 \cdot 10^6$.. $8 \cdot 10^6$	13092	32 bit real	0.050
ES8-V9	X component of satellite velocity at record start	m sec ⁻¹	$-1 \cdot 10^4$.. $1 \cdot 10^4$	13092	32 bit real	0.050
ES8-V10	X component of satellite velocity at record end	m sec ⁻¹	$-1 \cdot 10^4$.. $1 \cdot 10^4$	13092	32 bit real	0.050
ES8-V11	Y component of satellite velocity at record start	m sec ⁻¹	$-1 \cdot 10^4$.. $1 \cdot 10^4$	13092	32 bit real	0.050
ES8-V12	Y component of satellite velocity at record end	m sec ⁻¹	$-1 \cdot 10^4$.. $1 \cdot 10^4$	13092	32 bit real	0.050

Table 5-4. ES-8 Vdata Summary

Item	Parameter Name (Vdata Name)	Units	Range	Maximum Number of Vdata Elements	Data Type	Maximum Vdata Size (MB)
ES8-V13	Z component of satellite velocity at record start	m sec ⁻¹	-1.. 10^4 .. 1.. 10^4	13092	32 bit real	0.050
ES8-V14	Z component of satellite velocity at record end	m sec ⁻¹	-1.. 10^4 .. 1.. 10^4	13092	32 bit real	0.050
ES8-V15	Colatitude of satellite nadir at record start	deg	0 .. 180	13092	32 bit real	0.050
ES8-V16	Colatitude of satellite nadir at record end	deg	0 .. 180	13092	32 bit real	0.050
ES8-V17	Longitude of satellite nadir at record start	deg	0 .. 360	13092	32 bit real	0.050
ES8-V18	Longitude of satellite nadir at record end	deg	0 .. 360	13092	32 bit real	0.050
ES8-V19	Colatitude of Sun at observation	deg	0 .. 180	13092	32 bit real	0.050
ES8-V20	Longitude of Sun at observation	deg	0 .. 360	13092	32 bit real	0.050
ES8-V21	Spectral Response Functions:					
	SW channel wavelengths	μm	0 .. 200	632	32 bit real	0.002
	SW spectral response values	N/A	-1 .. 1	632	32 bit real	0.002
	TOT channel wavelengths	μm	0 .. 200	1051	32 bit real	0.004
	TOT spectral response values	N/A	-1 .. 1	1051	32 bit real	0.004
	WN channel wavelengths	μm	0 .. 200	871	32 bit real	0.003
	WN spectral response values	N/A	-1 .. 1	871	32 bit real	0.003
Total Vdata Size						1.12

5.4 Metadata

The CERES metadata are listed in [Table A-1](#) and [Table A-2](#) in [Appendix A](#). [Table A-1](#) lists the CERES Baseline Header Metadata and [Table A-2](#) lists the parameters in the Vdata Metadata Table. Note that the Vdata Metadata is a subset of the CERES Baseline Header Metadata.

6.0 Theory of Measurements and Data Manipulations

6.1 Theory of Measurements

See CERES ATBD Subsystem 2.0 (Reference 5).

6.2 Data Processing Sequence

The ERBE-like Inversion Subsystem (2.0) converts filtered radiometric measurements in engineering units received from the Instrument Subsystem (1.0) to instantaneous flux estimates at the TOA. This inversion process is dependent on several factors, including Earth surface features, the extent of cloudiness, and the relative geometry of the spacecraft, the sun, and the measurement FOV. Each radiometric measurement is spectrally corrected to give an unfiltered measurement. The observed scene is determined by a scene identification algorithm based on these unfiltered measurements, using angular distribution models and statistics provided by the CERES Science Team. Estimates of the radiant flux at the TOA are computed based on scene information, geometrical considerations, and the unfiltered measurements.

For detailed information see the ERBE-like Software Requirements Document (Subsystem 2.0) (Reference 6).

6.3 Special Corrections/Adjustments

Algorithms not discussed in the ATBD are discussed in this section.

7.0 Errors

See the Data Quality Summary

{URL=http://eosweb.larc.nasa.gov/project/ceres/ES8/disclaimer_CER_ES8.html}.

7.1 Quality Assessment

QA activities are performed at the Science Computing Facility by the Data Management Team. Processing reports containing statistics and processing results are examined for anomalies. If the reports show anomalies, data visualization tools are used to examine those products in greater detail to begin the anomaly investigation. (See the QA flag description for this product.)

7.2 Data Validation by Source

See Subsystem 2.0 Validation Document (Reference 7) for details on the data validation plan.

8.0 Notes

Notes are given to expand on subjects that will help in the use and understanding of the ES-8 product. These notes are generally characterized by more details and longer length than other definitions (See Section 4.3).

Note-1 Conversion of Julian Date to Calendar Date

The Julian Date is a time system that has been adopted by astronomers and is used in many scientific experiments. The Julian Date or Julian Day is the number of mean solar days since 1200 hours (GMT/UT/UTC/Zulu) on Monday, 24 November 4714 BCE, based on the current Gregorian calendar, or more precisely, the Gregorian Proleptic calendar. In other words, Julian day number 0 (zero) was Monday, 24 November 4714 BCE, 1200 hours (noon). A new Julian day starts when the mean Sun at noon crosses the Greenwich meridian. This differs from UT or Greenwich Mean Solar Time by 12 hours since UT changes day at Greenwich midnight. [Table 8-1](#) below provides Julian day numbers which relate UT to Julian date.

Important facts related to the Gregorian calendar are:

- a. There is no year zero; year -1 is immediately followed by year 1.
- b. A leap year is any year which is divisible by 4, except for those centesimal years (years divisible by 100) which must also be divisible by 400 to be considered a leap year.
- c. A leap year has 366 days, with the month of February containing 29 days.
- d. Year -1 is defined as a leap year, thus being also defined as containing 366 days, and being divisible by 4, 100, and 400.

Information on history, calendars, and Julian day numbers can be found in Blackadar's "A Computer Almanac" (See Reference 8) and on the WWW (See Reference 9).

The Julian day whole number is followed by the fraction of the day that has elapsed since the preceding noon (1200 hours UTC). The Julian Date JDATE can be represented as:

$$\text{JDATE} = \text{JDay} + \text{JFract}$$

where:

JDay = the integer Julian Day number and

JFract = the "fractional" Julian day (0 to 0.99...9)

(e.g. 245_0814.0 = 1200 or noon, 31 December, 1997 UT)

When the fractional part of the combined Julian date is .0, it is noon or 1200 hours GMT and when the fraction part is .5, then it is midnight or 0000 hours GMT.

The calculation of GMT (YYYYMMDD-HH:MM:SS.SSS) from Julian date (JDATE) is performed using the following process.

1. The YYYYMMDD can be determined using [Table 8-1](#) to find the year and the beginning of the month whose Julian Day occurs before the JDay integer value.
2. Calculate the number of days past the 0.5 day of the month via [Table 8-1](#) which provides Julian day numbers which relate UT to Julian date.

The GMT is determined by first computing the number of seconds in the day since midnight:

```

if   JFract > 0.5,
then Seconds = 86400.0 * (JFract-0.5)
if   JFract <= 0.5,
then Seconds = 86400.0 * (JFract+0.5)

```

Then compute HH, MM, and SS where:

```

HH = Int(Seconds/3600)
MM = Int(Seconds-(HH*3600.0)/60)
SS = Seconds-(HH*60.0 + MM)*60.0

```

As an example, if JD = 244_5733.5833, then the GMT date is computed using [Table 8-1](#) by finding the closest beginning monthly calendar noon date, which is Feb 0.5, 1984 (UT).

```

(Feb 0.5)      Jday
244_5731 < 244_5733.5833

```

JD = 244_5733.5833 is 2.5833 days past Feb 0.5, 1984 UT (i.e., past 1984 Jan 31^d 12^h 0^m 0^s) where 1984 Jan 31^d 12^h 0^m 0^s = (244_5733-244_5731).

Beginning with the whole days portion of 2.5833 (i.e., 2), the GMT Date is 1984 Jan 31^d 12^h 0^m 0^s + 2 = 1984 Feb 2^d 12^h 0^m 0^s.

Next, since JFract (0.5833) is > 0.5, 12^h is added to the GMT Date, yielding: 1984 Feb 2^d 12^h 0^m 0^s + 12^h 0^m 0^s = 1984 Feb 3^d 0^h 0^m 0^s.

Finally, to get the GMT time and since JFract (0.5833) is > 0.5, the number of seconds = 86400 * (0.5833 - 0.5) = 7197.12 yielding:

```

HH = 7197.12 / 3600 = 01.9992 = 01h
MM = 7197.12 - ((1*3600) / 60) = 59.952 = 59m
SS = 7197.12 - ((1*60) + 59)*60 = 57.12s

```

Therefore, the GMT Date corresponding to the Julian Date 244_5733.5833 = 1984 Feb 3^d 1^h 59^m 57.12^s, which is UT = 1984 Jan 31^d 12^h 0^m 0^s + 2.5833 days.

Table 8-1. Julian Day Number

Year	Jan 0.5a	Feb 0.5	Mar 0.5	Apr 0.5	May 0.5	June 0.5	July 0.5	Aug 0.5	Sept 0.5	Oct 0.5	Nov 0.5	Dec 0.5
1980t	244_4239	_4270	_4299	_4330	_4360	_4391	_4421	_4452	_4483	_4513	_4544	_4574
1981	_4605	_4636	_4664	_4695	_4725	_4756	_4786	_4817	_4848	_4878	_4909	_4939
1982	_4970	_5001	_5029	_5060	_5090	_5121	_5151	_5182	_5213	_5243	_5274	_5304
1983	_5335	_5366	_5394	_5425	_5455	_5486	_5516	_5547	_5578	_5608	_5639	_5669
1984t	_5700	_5731	_5760	_5791	_5821	_5852	_5882	_5913	_5944	_5974	_6005	_6035
1985	244_6066	_6097	_6125	_6156	_6186	_6217	_6247	_6278	_6309	_6339	_6370	_6400
1986	_6431	_6462	_6490	_6521	_6551	_6582	_6612	_6643	_6674	_6704	_6735	_6765
1987	_6796	_6827	_6855	_6886	_6916	_6947	_6977	_7008	_7039	_7069	_7100	_7130
1988t	_7161	_7192	_7221	_7252	_7282	_7313	_7343	_7374	_7405	_7435	_7466	_7496
1989	_7527	_7558	_7586	_7617	_7647	_7678	_7708	_7739	_7770	_7800	_7831	_7861
1990	244_7892	_7923	_7951	_7982	_8012	_8043	_8073	_8104	_8135	_8165	_8196	_8226
1991	_8257	_8288	_8316	_8347	_8377	_8408	_8438	_8469	_8500	_8530	_8561	_8591
1992t	_8622	_8653	_8682	_8713	_8743	_8774	_8804	_8835	_8866	_8896	_8927	_8957
1993	_8988	_9019	_9047	_9078	_9108	_9139	_9169	_9200	_9231	_9261	_9292	_9322
1994	_9353	_9384	_9412	_9443	_9473	_9504	_9534	_9565	_9596	_9626	_9657	_9687
1995	244_9718	_9749	_9777	_9808	_9838	_9869	_9899	_9930	_9961	_9991	*0022	*0052
1996t	245_0083	_0114	_0143	_0174	_0204	_0235	_0265	_0296	_0327	_0357	_0388	_0418
1997	_0449	_0480	_0508	_0539	_0569	_0600	_0630	_0661	_0692	_0722	_0753	_0783
1998	_0814	_0845	_0873	_0904	_0934	_0965	_0995	_1026	_1057	_1087	_1118	_1148
1999	_1179	_1210	_1238	_1269	_1299	_1330	_1360	_1391	_1422	_1452	_1483	_1513
2000t	245_1544	_1575	_1604	_1635	_1665	_1696	_1726	_1757	_1788	_1818	_1849	_1879
2001	_1910	_1941	_1969	_2000	_2030	_2061	_2091	_2122	_2153	_2183	_2214	_2244
2002	_2275	_2306	_2334	_2365	_2395	_2426	_2456	_2487	_2518	_2548	_2579	_2609
2003	_2640	_2671	_2699	_2730	_2760	_2791	_2821	_2852	_2883	_2913	_2944	_2974
2004t	245_3005	_3036	_3065	_3096	_3126	_3157	_3187	_3218	_3249	_3279	_3310	_3340
2005	_3371	_3402	_3430	_3461	_3491	_3522	_3552	_3583	_3614	_3644	_3675	_3705
2006	_3736	_3767	_3795	_3826	_3856	_3887	_3917	_3948	_3979	_4009	_4040	_4070
2007	_4101	_4132	_4160	_4191	_4221	_4252	_4282	_4313	_4344	_4374	_4405	_4435
2008t	245_4466	_4497	_4526	_4557	_4587	_4618	_4648	_5679	_4710	_4740	_4771	_4801
2009	_4832	_4863	_4891	_4922	_4952	_4983	_5013	_5044	_5075	_5105	_5136	_5166

a. Jan. 0.5 (UT) is the same as Greenwich noon (12h) UT, Dec. 31. * These dates begin with 245 t Denotes leap years

Note-2 Colatitude and Longitude of Nadir

The colatitude and longitude of the satellite nadir (See [Term-11](#)) at the start of the record are determined as follows. The position of the satellite is

$$x = (\text{ES8-V3})$$

$$y = (\text{ES8-V5})$$

$$z = (\text{ES8-V7})$$

and the radius is $r = \sqrt{x^2 + y^2 + z^2}$ so that the colatitude (See [Figure 4-1](#)) is

$$\Theta = \cos^{-1}\left(\frac{z}{r}\right) \quad 0^\circ \leq \Theta \leq 180^\circ$$

The projection of the radius on the equatorial plane is $r_{eq} = \sqrt{x^2 + y^2}$ so that the longitude is

$$\cos \Phi = \frac{x}{r_{eq}}$$

$$\sin \Phi = \frac{y}{r_{eq}}$$

$$\Phi = \tan^{-1}\left(\frac{\sin \Phi}{\cos \Phi}\right) \quad 0^\circ \leq \Phi \leq 360^\circ$$

The colatitude and longitude at the end of the record is determined in a similar way with [ES8-V4](#), [ES8-V6](#), and [ES8-V8](#).

Note-3 CERES Point Spread Function

Note-3.1 CERES Point Spread Function

The CERES scanning radiometer is an evolutionary development of the ERBE scanning radiometer. It is desired to increase the resolution as much as possible, using a thermistor bolometer as the detector. As the resolution is increased, the sampling rate must increase to achieve spatial coverage. When the sampling rate becomes comparable to the response time of the detector, the effect of the time response of the detector on the PSF must be considered. Also, the signal is usually filtered electronically prior to sampling in order to attenuate electronic noises and to remove high frequency components of the signal which would cause aliasing errors. The time response of the filter, together with that of the detector causes a lag in the output relative to the input radiance. This time lag causes the centroid of the PSF to be displaced from the centroid of the optical FOV. Thus, the signal as sampled comes not only from where the radiometer is pointed, but includes a “memory” of the input from where it had been looking. Another effect of the time response is to broaden the PSF, which will reduce the resolution of the measurement, increase blurring errors, and decrease aliasing errors.

Note-3.2 Geometry of the Point Spread Function

The scanner footprint geometry is given in [Figure 8-1](#). The optical FOV is a truncated diamond (or hexagon) and is 1.3° in the along-scan direction and 2.6° in the across-scan direction. The

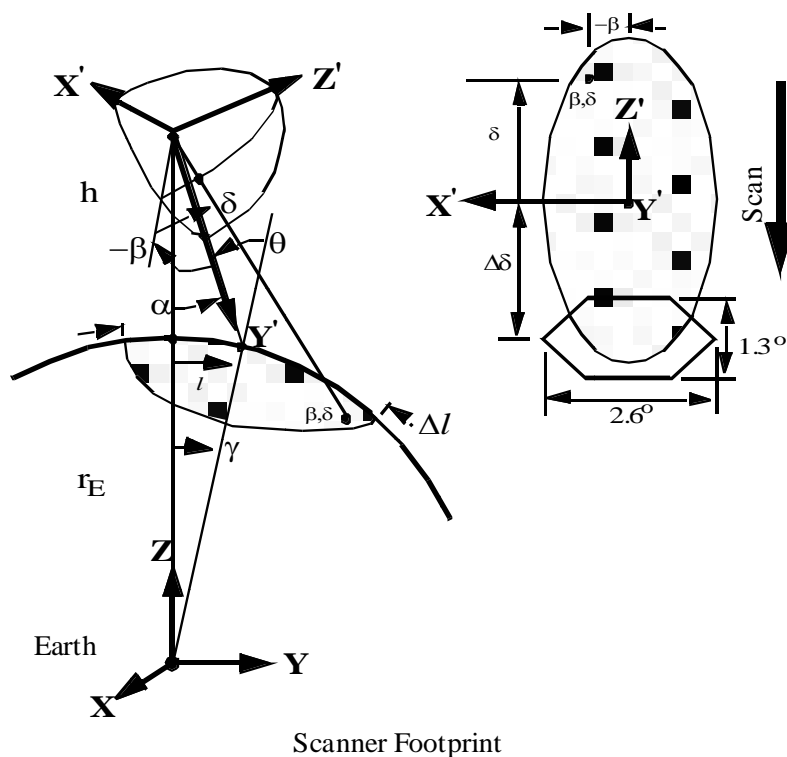


Figure 8-1. Scanner Footprint

effective FOV (or footprint) is given by the PSF and is shown as an ellipse. A point within the footprint is located by β and δ . The cone angle α (or nadir angle) determines the location of the footprint centroid on the Earth. If $\alpha = 0$, the footprint is at nadir. The viewing zenith angle θ is a direct result of the satellite altitude h , the Earth radius r_E , and the cone angle α . The surface distance l and the Earth central angle γ between nadir and the centroid are also a result of the viewing geometry. In [Figure 8-1](#) we have denoted the length of the FOV by Δl .

Note-3.3 Analytic form of the Point Spread Function

A full discussion of an analytic model of the point spread function and its development is given in Smith (See Reference 10). From Figure 8-1, we redraw half of the optical FOV in Figure 8-2

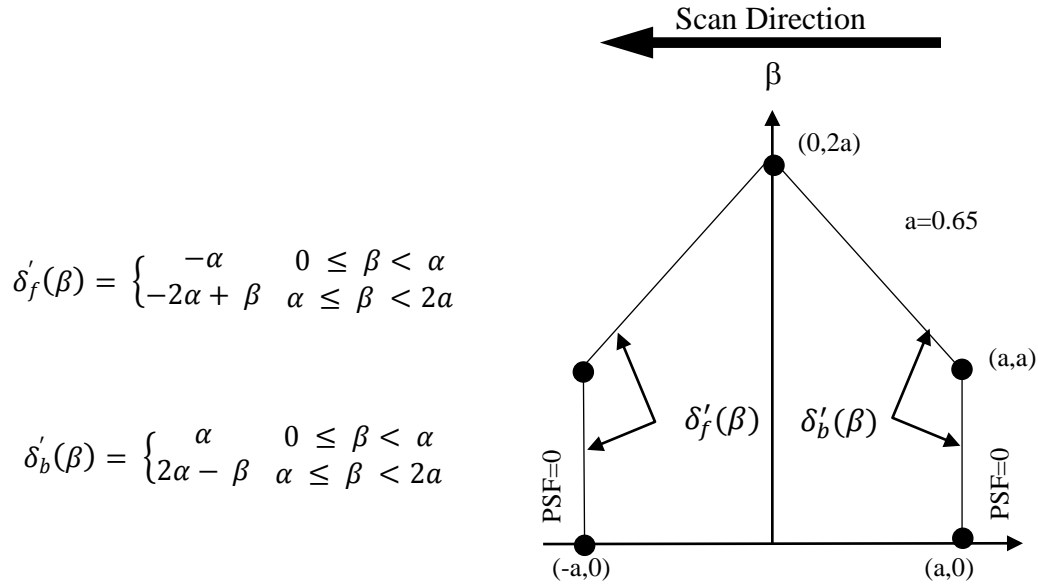


Figure 8-2. Optical FOV

where δ' is the along-scan angle and β is the cross-scan angle. Note that δ' points opposite the scan direction and increases toward the tail of the PSF (See Figure 8-3). The forward and back boundaries y and x , respectively. With these definitions the CERES PSF are given by $\delta'_f(\beta)$ and $\delta'_b(\beta)$, respectively. With these definitions the CERES PSF is written as

$$P(\delta', \beta) = \begin{cases} 0 & |\beta| > 2\alpha \\ 0 & \delta' < \delta'_f(\beta) \\ F[\delta' - \delta'_f(\beta)] & \delta'_f(\beta) \leq \delta' < \delta'_b(\beta) \\ F[\delta' - \delta'_f(\beta)] - F[\delta' - \delta'_b(\beta)] & (\text{otherwise}) \end{cases} \quad (1)$$

where

$$\begin{aligned} F(\xi) = & 1 - (1 + a_1 + a_2)e^{-1.78348\xi} \\ & + e^{-3.04050\xi}[a_1 \cos(0.91043\xi) + b_1 \sin(0.91043\xi)] \\ & + e^{-2.20860\xi}[a_2 \cos(2.78981\xi) + b_2 \sin(2.78981\xi)] \end{aligned} \quad (2)$$

and

$$a_1 = 5.83761 \quad a_2 = -0.18956$$

$$b_1 = 2.87362 \quad b_2 = 1.02431$$

where ξ is in degrees and (0.91043ξ) and (2.78981ξ) are in radians. The centroid of the PSF is derived in Smith (See Reference 10) and is 1.51° from the optical axis. This shift is denoted in Figure 8-3 and a new angle δ is defined relative to the centroid. To evaluate the PSF we determine δ and then set $\delta' = \delta + \delta_0$ where δ_0 is the shift (or offset) from the optical axis to the centroid.

The numerical values given in equation (1) are based on the following prelaunch calibration constants:

$$f_c = 10.5263 \text{ hertz}$$

Characteristic frequency of the Bessel Filter

$$\tau = 0.0089 \text{ sec}$$

Detector time constant

$$\dot{\alpha} = 63.0 \text{ deg/sec}$$

Scan rate

Table must be from BDS - check for any text that goes with (currently no reference to Table 8-2)

Table 8-2. Detector Time Constant (τ seconds)

Instrument	Detector Channel		
	Total	Window	Shortwave
PFM	0.00860	0.00830	0.00815
FM1	0.00850	0.00795	0.00825
FM2	0.00800	0.00820	0.00820
FM3	0.00888	0.00868	0.00838
FM4	0.00928	0.00858	0.00888

The general form of equation (1) is given by

$$\begin{aligned}
F(\xi) = & 1 - (1 + a_1 + a_2)e^{-\eta t} \\
& + e^{\mu_1 t} [a_1 \cos(\omega_1 t) + b_1 \sin(\omega_1 t)] \\
& + e^{\mu_2 t} [a_2 \cos(\omega_2 t) + b_2 \sin(\omega_2 t)]
\end{aligned} \tag{3}$$

where

$$t = \frac{2\pi f_c}{\dot{\alpha}} \xi$$

and where the complex roots of the 4-pole Besssel filter are

$$\begin{aligned}
v_1 &= -2.89621 + 0.86723i = \mu_1 + i\omega_1 \\
v_2 &= -2.10379 + 2.65742i = \mu_2 + i\omega_2
\end{aligned}$$

the residues of the Bessel filter are

$$\begin{aligned}
u_1 &= +1.66339 - 8.39628i \\
u_2 &= -1.66339 + 2.24408i
\end{aligned}$$

and

$$\eta = \frac{1}{2\pi f_c \tau}$$

Note that ω_i, η , and t are non-dimensional so that $(\omega_i t)$ is in radians. The cone angle ξ has units of degrees. The complex variables p_i, v_i, u_i define a_i and b_i as

$$p_i = \frac{u_i}{\eta + v_i}, \quad a_i = 2\eta \operatorname{Re}\left(\frac{p_i}{v_i}\right), \quad b_i = -2\eta \operatorname{Im}\left(\frac{p_i}{v_i}\right) \quad i = 1, 2,$$

The centroid of the PSF can be derived from the analytic expression and is given by

$$\delta_0 = \dot{\alpha} \tau (1 + \eta) \tag{4}$$

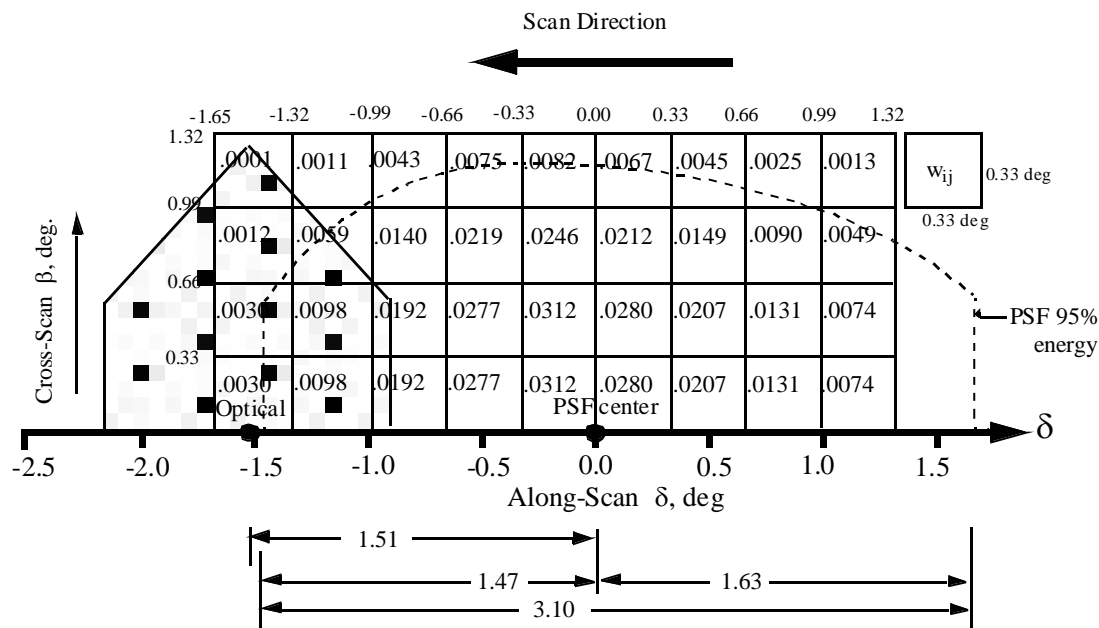


Figure 8-3. TRMM Angular Bin Weights

Note-4 Definition of Angular Distribution Models (ADM)

The angular distribution model, $R(\theta, \phi)$, is a function of the viewing zenith angle, θ , and relative azimuth angle, ϕ , (See Figure 4-2) and defines the functional relationship between flux, F , and radiance, I , as

$$I(\theta, \phi) = \pi^{-1} F R(\theta, \phi) \quad (5)$$

Let us integrate radiance I in (5) over the hemisphere to get flux F , or

$$\int_0^{2\pi} \int_0^{\pi/2} I(\theta, \phi) \cos \theta \sin \theta d\theta d\phi = \pi^{-1} F \int_0^{2\pi} \int_0^{\pi/2} R(\theta, \phi) \cos \theta \sin \theta d\theta d\phi \quad (6)$$

or

$$\pi^{-1} \int_0^{2\pi} \int_0^{\pi/2} R(\theta, \phi) \cos \theta \sin \theta d\theta d\phi = 1 \quad (7)$$

which establishes a normalization for $R(\theta, \phi)$. It is common to assume R is independent of azimuth for longwave radiance so that the normalization (7) reduces to

$$2 \int_0^{\pi/2} R(\theta) \cos \theta \sin \theta d\theta = 1 \quad (8)$$

The main purpose for modeling anisotropy as $R(\theta, \phi)$ is to estimate flux from measured radiance by (5) as

$$\hat{F} = \frac{\pi^{-1} I(\theta, \phi)}{R(\theta, \phi)} \quad (9)$$

$R(\theta, \phi)$ is also a function of other angles and scene types such as land, ocean, cloud cover, optical depth, etc. For shortwave, $R_i(\theta, \phi, \theta_o)$ denotes R is a function of the solar zenith angle, θ_o , (See Figure 4-2) and scene type i (See ES8-14). When constructing R from data, we sort the data into scene types and assume R is piecewise constant over angular bins. When evaluating R for specific angles (θ, ϕ, θ_o) we assume R is piecewise linear and use a tri-linear interpolation and a slightly different normalization constant. There is no interpolation between scene types. For longwave, $R_i(\theta, \Theta)$ denotes R is a function of colatitude, Θ , and scene type i . Construction and evaluation is the same as for shortwave.

Note-5 Maximum Likelihood Estimator (MLE) of Scene Type

The Maximum Likelihood Estimator (MLE) is a bi-spectral identifier of cloud cover where clouds are characterized as cold and bright. Based on the unfiltered shortwave and longwave scanner measurements

$$I^{\text{SW}} = (\text{ES8-9})$$

$$I^{\text{LW}} = (\text{ES8-10})$$

the scene corresponding to each scanner measurement is identified as one of four cloud conditions over a predetermined geographic or surface type. The first step is to determine the 2.5° region that contains the scanner TOA point (See Term-23) given by ES8-1 and ES8-2. From a priori physical data, we then determine the geographic scene as either ocean, land, snow, desert, or land-ocean mix. Next we determine the cloud condition. An example of a typical scene identification is shown in Figure 8-4.

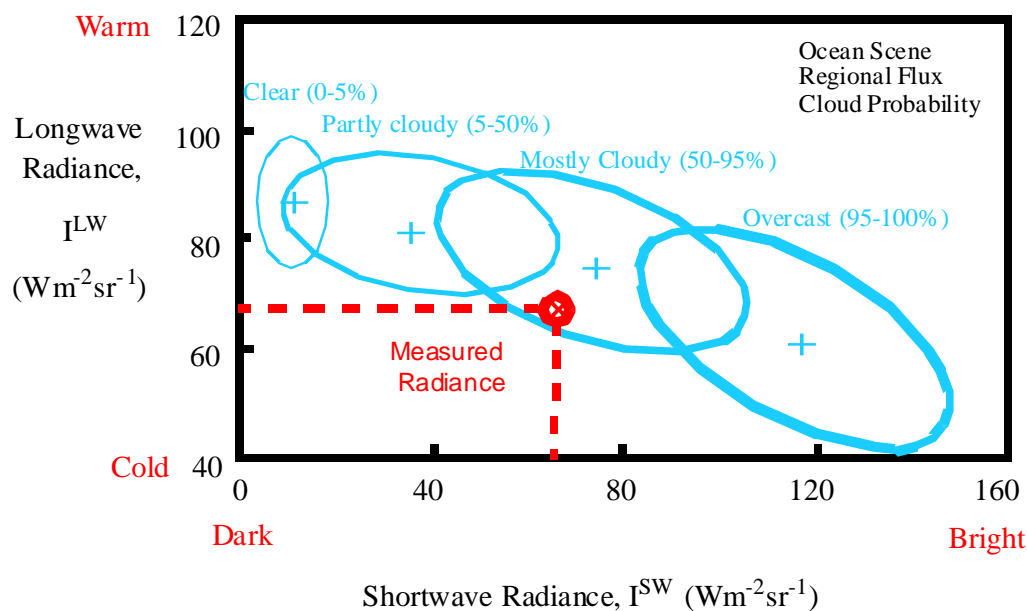


Figure 8-4. ERBE Scene Identification Algorithm

Knowing the geographic scene and the directional angles [ES8-6](#), [ES8-7](#), and [ES8-8](#), we can evaluate from a priori data the measurements we would expect from a clear sky, partly cloudy, mostly cloudy, and overcast conditions. The ellipse about each point represents the variance we would expect. The identification consists of determining which one of the four cloud conditions is the closest to the actual measurement point in a probabilistic sense. The details of the MLE are given by Wielicki and Green (Reference [12](#)).

Note-6 Spectral Correction Algorithm

The radiances as measured by the CERES instruments are filtered radiances and the spectral correction algorithm unfilters these radiances. The desired unfiltered radiances are defined by

$$I^{SW} = \int_0^{\infty} I_{\lambda}^r d\lambda$$

$$I^{LW} = \int_0^{\infty} I_{\lambda}^e d\lambda$$

$$I^{WN} = \frac{1}{\lambda_2 - \lambda_1} \int_{\lambda_1}^{\lambda_2} I_{\lambda}^e d\lambda$$

where λ (μm) is the wavelength, $\lambda_1 = 8.1$ and $\lambda_2 = 11.8$, and I_λ^r and I_λ^e are the reflected and emitted components of the total observed radiance or $I_\lambda = I_\lambda^r + I_\lambda^e$. The filtered measurements are modeled as

$$m_f^i = \int_0^\infty S_\lambda^i I_\lambda d\lambda \quad i = SW, TOT$$

$$m_f^i = \frac{1}{\lambda_2 - \lambda_1} \int_0^\infty S_\lambda^i I_\lambda d\lambda \quad i = WN$$

where S_λ^i is the normalized spectral response function ($0 \leq S_\lambda^i \leq 1$). The spectral response function for CERES_ TRMM is shown in the [Figure 8-5](#) and represents the spectral throughput of the individual detector's optical elements determined from laboratory measurements. An estimate of the unfiltered SW and WN radiances are determined from the filtered radiance measurements as follows:

$$\hat{f}^{SW} = a_0 + a_1 (m_f^{SW_r}) + a_2 (m_f^{SW_r})^2$$

$$\hat{f}^{WN} = b_0 + b_1 (m_f^{WN}) + b_2 (m_f^{WN})^2$$

where a_0, a_1, a_2, b_0, b_1 , and b_2 are theoretically derived regression coefficients that depend on scene type and viewing geometry. $m_f^{SW_r}$ represents the reflected portion of the filtered SW radiance measurement and is given by $m_f^{SW_r} = m_f^{SW} - m_f^{SW_e}$ where $m_f^{SW_e}$ is the emitted thermal portion of m_f^{SW} and is estimated from m_f^{WN} using a pre-determined empirical 2nd order polynomial expression relating nighttime m_f^{SW} and m_f^{WN} measurements. For CERES_ TRMM the least-square fit is given by:

$$m_f^{SW_e} = k_0 + k_1 (m_f^{WN}) + k_2 (m_f^{WN})^2$$

where $k_0 = 0.1208$, $k_1 = -0.001697$, and $k_2 = 0.0006875$. Since there are no filtered longwave radiance measurements in CERES, the unfiltered emitted LW radiance must be inferred from measurements in the other available channels. An estimate of the daytime (D) and nighttime (N) LW radiance is given by

$$\hat{f}^{LW}(D) = c_0 + c_1 m_f^{SW_r} + c_2 m_f^{TOT} + c_3 m_f^{WN}$$

$$\hat{f}^{LW}(N) = d_0 + d_1 m_f^{TOT} + d_2 m_f^{WN}$$

where the c and d coefficients are theoretically derived regression coefficients. All of the spectral correction coefficients (SCC) are obtained from a regression analysis of theoretically derived filtered and unfiltered radiances in each channel. The simulated radiances are inferred from a spectral radiance database of typical Earth scenes and the spectral response functions. Each CERES instrument has its own set of SCC based on its spectral response. There are different SCC for land, ocean, snow, and cloud. The SCC also vary with solar zenith, viewing zenith, and relative azimuth. Additional details are given in Reference [13](#).

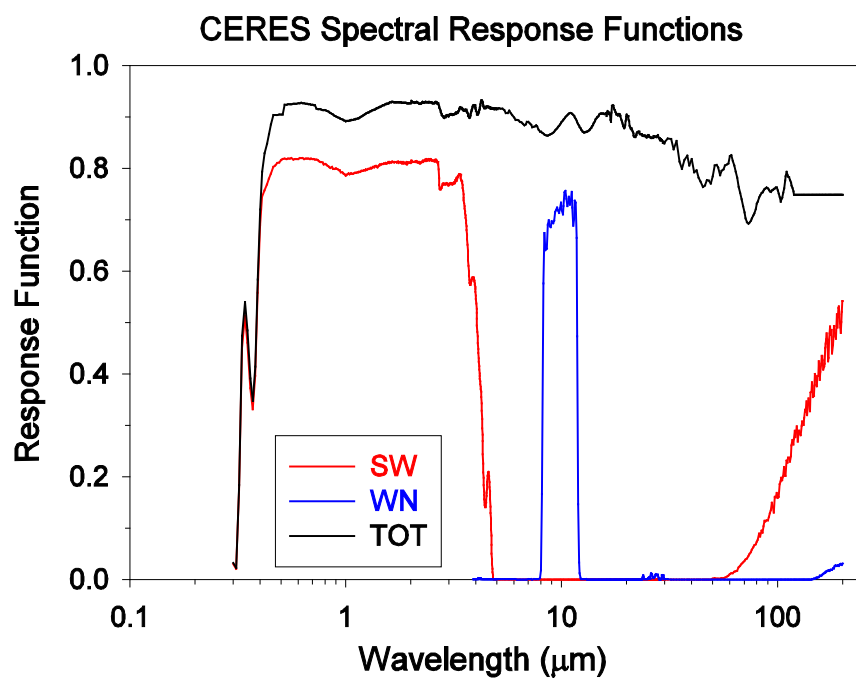


Figure 8-5. CERES TRMM Spectral Response

9.0 Application of the Data Set

The ES-8 data product provides time and position data on a record-level basis and measurement-level data including filtered, unfiltered, TOA, and scene identification data (See Section [1.4](#)).

10.0 Future Modifications and Plans

Modifications to the ES-8 product are driven by validation results and any Terra related parameters. The Langley ASDC provides users notification of changes.

11.0 Software Description

There are Fortran90 and C read programs available at the Langley ASDC. The programs were designed to run on a Unix workstation and can be compiled with a Fortran90 or C compiler, respectively.

{Pointer to ASDC read program}

12.0 Contact Data Center/Obtain Data

NASA Langley Atmospheric Sciences Data Center
Science, User and Data Service Office
NASA Langley Research Center
Mail Stop 157D
2 South Wright Street
Hampton, VA 23681-2199
USA

Telephone: (757) 864-8656
FAX: (757) 864-8807
E-mail: larc@eos.nasa.gov
URL: <http://eosweb.larc.nasa.gov/>

13.0 Output Products and Availability

Several media types are supported by the Langley Web Order Tool. Data can be downloaded from the Web or via FTP. Alternatively, data can be ordered on media tapes. The media tapes supported are 4mm 2Gb (90m), 8mm 2Gb (8200), 8mm 5Gb (8500), and 8mm 7Gb (8500c).

Data ordered via the Web or via FTP can be downloaded in either Uncompressed mode or in UNIX Compressed mode. Data written to media tape (in either Uncompressed mode or in UNIX Compressed mode) is in UNIX TAR format.

14.0 References

1. NASA Langley Atmospheric Science Data Hierarchical Data Format Web site {[URL = https://eosweb.larc.nasa.gov/HBDOCS/hdf.html](https://eosweb.larc.nasa.gov/HBDOCS/hdf.html)}.
2. Clouds and the Earth's Radiant Energy System (CERES) Data Management System Data Products Catalog Release 3, Version 1, July 1998 {[URL = http://ceres.larc.nasa.gov/dpc_current.php](http://ceres.larc.nasa.gov/dpc_current.php)}.
3. TRW DRL 64, 55067.300.008E; In-flight Measurement Analysis (Rev. E), March 1997.
4. Clouds and the Earth's Radiant Energy System (CERES) Algorithm Theoretical Basis Document, Instrument Geolocate and Calibrate Earth Radiances (Subsystem 1.0), Release 2.2, June 1997 {[URL = http://ceres.larc.nasa.gov/atbd.php](http://ceres.larc.nasa.gov/atbd.php)}.
5. Clouds and the Earth's Radiant Energy System (CERES) Algorithm Theoretical Basis Document, ERBE-like to Instantaneous Fluxes (Subsystem 2.0), Rel. 2.2, June 2, 1997 {[URL = http://ceres.larc.nasa.gov/atbd.php](http://ceres.larc.nasa.gov/atbd.php)}.
6. Clouds and the Earth's Radiant Energy System (CERES) Data Management System Software Requirements Document, ERBE-like Inversion to Instantaneous TOA and Surface Fluxes (Subsystem 2.0), Release 1 Version 1, November 1994 {[URL = http://ceres.larc.nasa.gov/srd.php](http://ceres.larc.nasa.gov/srd.php)}.
7. Clouds and the Earth's Radiant Energy System (CERES) Validation Plan, ERBE-like Inversion to Instantaneous TOA Flux (Subsystem 2.0), Release 2.2, July 1997 {[URL = http://ceres.larc.nasa.gov/validation.php](http://ceres.larc.nasa.gov/validation.php)}.
8. Blackadar, Alfred: A Computer Almanac, Weatherwise, Vol 37, No 5, October 1984, p. 257-260.
9. Jefferys, William H.: Julian Day Numbers {[URL = http://quasar.as.utexas.edu/BillInfo/JulianDatesG.html](http://quasar.as.utexas.edu/BillInfo/JulianDatesG.html)}.
10. Smith, G. L., 1994: Effects of time response on the point spread function of a scanning radiometer, *Appl. Opt.*, Vol. 33, No. 30, 7031-7037.
11. Software Bulletin "CERES Metadata Requirements for LaTIS," Revision 1, January 7, 1998 {[URL = http://ceres.larc.nasa.gov/sw_bull.php](http://ceres.larc.nasa.gov/sw_bull.php)}.
12. Wielicki, B. A., and R. N. Green, 1989: Cloud identification for ERBE radiation flux retrieval, *J. Appl. Meteor.*, **28**, 1133-1146.
13. Loeb, N. G., Priestley, K. J., Kratz, D. P., Geier, E. B., Green, R. N., Wielicki, B. A., Hinton, P. O R., and Nolan, S. K.: Determination of Unfiltered Radiances from CERES. Submitted to *Journal of Applied Meteorology*, 2000.

15.0 Glossary of Terms

Term-1 Cone Angle

The cone angle (See [Figure 15-1](#)) is the angle between a vector from the satellite to the center of the Earth and the instrument view vector from the satellite to the TOA point (See [Term-23](#)).

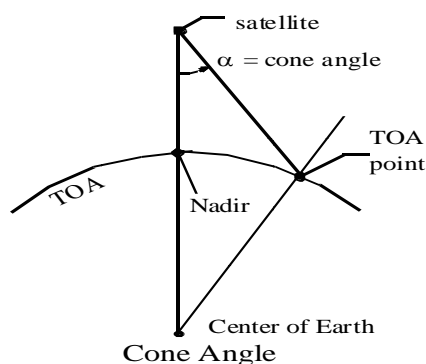


Figure 15-1. Cone Angle

Term-2 Count Conversion

Conversion from instrument counts to engineering units by a count conversion equation (See Reference 4 and BDS Collection Guide, Note 1).

Term-3 Earth Equator, Greenwich Meridian System

The Earth equator, Greenwich meridian system is an Earth-fixed, geocentric, rotating coordinate system with the X-axis in the equatorial plane through the Greenwich meridian, the Y-axis lies in the equatorial plane 90° to the east of the X-axis, and the Z-axis is toward the North Pole.

Term-4 Earth Surface

The surface of the Earth as defined by the WGS-84 Earth Model. The WGS-84 model of the Earth surface is an ellipsoid $\frac{x^2}{a^2} + \frac{y^2}{a^2} + \frac{z^2}{b^2} = 1$ where $a = 6378.1370$ km and $b = 6356.7523$ km (See [Figure 15-2](#)).

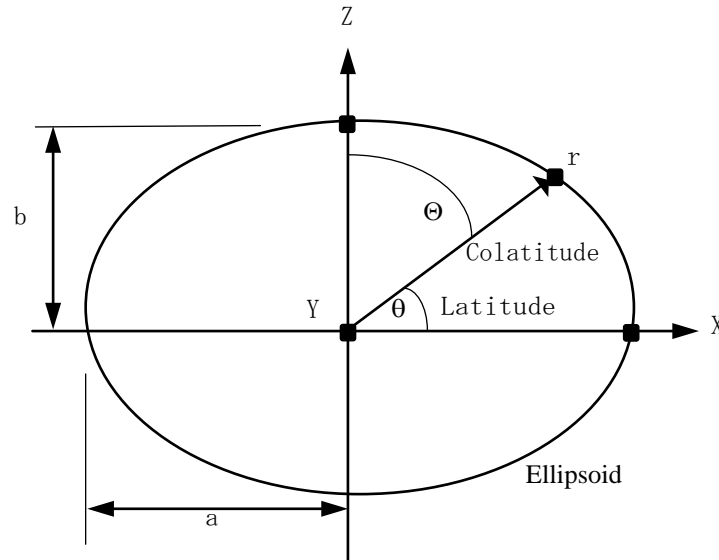


Figure 15-2. Ellipsoidal Model

We can determine the radial distance r as a function of the geocentric latitude θ by setting $x = r \cos(\theta)$, $y = 0$, $z = r \sin(\theta)$ in the ellipsoidal model and solving for r or $r = \frac{ab}{\sqrt{a^2 \sin^2 \theta + b^2 \cos^2 \theta}}$

Term-5 Elevation Angle

The elevation angle defines the position of the instrument optical axis (See [Note-3](#)) relative to the spacecraft. For nominal satellite attitude control, the elevation is near 90° for a nadir view (See [Term-11](#)), near 0° at the start of a 6.6 sec scan cycle, and near 180° at internal calibrations. Zero elevation is generally away from the Sun and 180° is generally on the sun side of the satellite.

Term-6 Field-of-View

The instrument field-of-view (FOV) is determined by the instrument point spread function (See [Term-12](#)) and is defined as the minimum area over the radiation field from which 95% of the measured radiance is obtained. For the purpose of determining full FOV coverage of the Earth surface (See [ES8-18](#)), the forward edge of the FOV is offset 1.7 deg at the satellite in front of the PSF centroid while the trailing edge is offset 1.7 deg behind the centroid. (See [Note-3](#)).

Term-7 Fixed azimuth plane scan (FAPS)

Term-8 Geocentric Colatitude

Term-9 Granule

The ES-8 product is one day or 24 hours of data and is called a granule. Or, a granule is all records (See [Term-14](#)) for a day.

Term-10 Julian Date

Julian Date is a continuous count of time in whole and fractional days elapsed at the Greenwich meridian since noon on January 1, 4714 BCE. (See [Note-1](#))

Term-11 Nadir

The point on the Earth surface below the satellite or the intersection point of a line from the center of the Earth to the satellite and the Earth surface (See [Figure 15-1](#)).

Term-12 Point Spread Function

A Point Spread Function (PSF) is a two-dimensional bell-shaped function that defines the CERES instrument response to the viewed radiation field. Due to the response time, the radiometer responds to a larger FOV than the optical FOV and the resulting PSF centroid lags the optical FOV centroid by more than a degree of cone angle (See [Term-1](#)) for normal scan rates (See [Note-3](#)).

Term-13 Rapid Retrace (or Fast Return)

Rapid retrace is defined as a much faster than nominal elevation, or cone angle, scan rate. The rapid retrace rate is currently defined as $249.69 \pm 10 \text{ deg sec}^{-1}$. During the Short Elevation Scan cycle, there are two portions of the scan cycle where the CERES instrument sweeps across the Earth at a rate of approximately 249 deg sec^{-1} . These are examples of rapid retrace (See [Figure 15-3](#)).

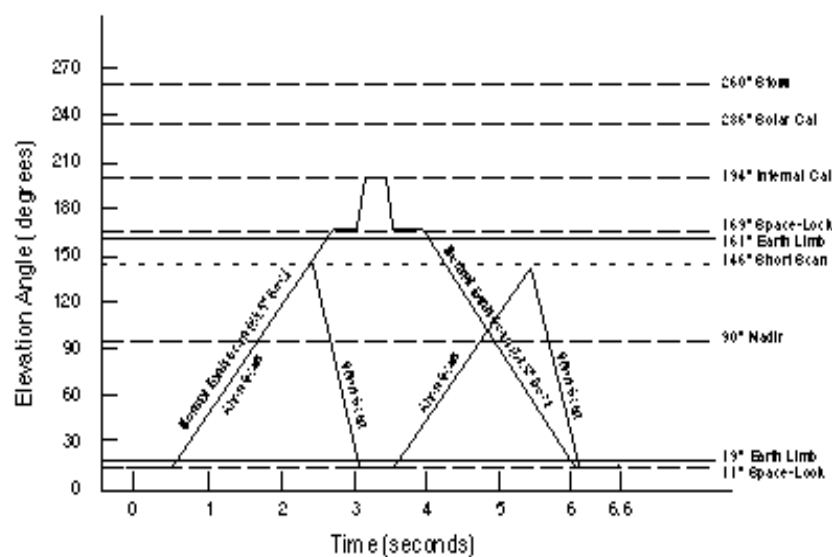


Figure 15-3. Normal and short Earth scan profiles for instrument on TRMM platform

Term-14 Record

A record contains data from one complete scan cycle of 6.6 sec (See [Term-17](#)). The records are ordered and numbered in time from 1 to a maximum of 13,092 (note: since the time length of a record may vary, the maximum number of records on the ES-8 can be 13,092). The record number is one of the dimension indices of the HDF output arrays.

Term-15 Resolution**Term-16 Rotation Azimuth Plane Scan (RAPS)****Term-17 Scan Cycle**

Each scan cycle is 6.6 sec in length and contains 660 measurement points so that measurements are every 0.01 sec. The beginning of a scan cycle is at measurement 1. The end of a cycle is 6.6 sec later at measurement 1 of the next cycle. The last measurement in the scan cycle is 660 and is 6.59 sec after measurement 1.

Term-18 Scan Sample Number

Each of the 660 measurements or samples within a scan cycle (See [Term-17](#)) is ordered and numbered in time from 1 to 660. The scan sample number is also one of the dimension indices of the HDF output arrays.

Term-19 Scientific Data Set

A Scientific Data Set (SDS) is an HDF structure. It is a collection (or grouping) of parameters that have the same data type such as 8, 16, or 32-bit integers or 32, or 64-bit floating point numbers. The ES-8 SDS's each contain only one parameter. The SDS is an array of values and for ES-8 this corresponds to a two dimensional array of all values of a certain parameter for a day. The dimensions of the array correspond to the number of footprints (660) within a record (scan cycle) and the number of records within the granule. In general, an SDS is a multi-dimensional array. It has dimension records and data type which describe it. The dimensions specify the shape and size of the SDS array. Each dimension has its own attributes.

Term-20 Spectral Correction

The Spectral Correction Coefficients (SCC) represent a regression between theoretical filtered radiances and theoretical unfiltered radiances and are used to unfilter the CERES radiances. Each CERES instrument has its own set of SCC based on its spectral response. There are different SCC for land, ocean, snow, and cloud. The SCC also vary with solar zenith, viewing zenith, and relative azimuth. (See [Note-6](#))

Term-21 Subsolar Point

The point at which a vector from the center of the Earth to the Sun intersects the TOA (See [Term-22](#)).

Term-22 Top-of-the-Atmosphere

The Top-of-the-Atmosphere (TOA) is a surface approximately 30 km above the Earth surface (See [Term-4](#)). Specifically, the TOA is an ellipsoid $\frac{x^2}{a^2} + \frac{y^2}{a^2} + \frac{z^2}{b^2} = 1$ where $a = 6408.1370$ km and $b = 6386.6517$ km (See [Figure 15-2](#)). We can determine the radial distance r as a function of the geocentric latitude θ_c by setting $x = r \cos(\theta)$, $y = 0$, $z = r \sin(\theta)$ in the ellipsoidal model and solving for r or

$$r = \frac{ab}{\sqrt{a^2 \sin^2 \theta + b^2 \cos^2 \theta}}$$

Term-23 TOA Point

The viewed point at the TOA, or the point at which the PSF (See [Term-12](#)) centroid intersects the TOA (See [Term-22](#)).

Term-24 Vertex Data

A Vertex data (Vdata) set is an HDF structure. It is a collection (or grouping) of parameters that have different data types such as 8, 16, or 32-bit integers, floating point numbers, text, etc. In general, Vdata is a table of parameters of varying data type. Specifically stated, a Vdata is a customized table, comprised of a collection of similar records (rows) whose values are stored in one or more fixed length fields (columns) where individual fields can have their own data type. The ES-8 contains 20 record-level parameters, each of which is written into a separate Vdata. Therefore, an ES-8 record-level Vdata contains a single field (column) which has multiple values (rows) such that one value exists for each record (scan cycle) within the granule. The ES-8 also contains a CERES_metadata Vdata which contains numerous parameters (columns) and each parameter has only one value per granule. A Vdata is uniquely identified by a name, a class, and individual field names. The Vdata class identifies the purpose or use of its data.

16.0 Acronyms and Units

16.1 CERES Acronyms

ADM	Angular Distribution Model
APID	Application Identifier
APD	Aerosol Profile Data
ATBD	Algorithm Theoretical Basis Document
AVG	Monthly Regional Radiative Fluxes and Clouds
AVHRR	Advanced Very High Resolution Radiometer
BCE	Before Current Era
BDS	BiDirectional Scan (data product)
CADM	CERES Angular Distribution Model
CER	CERES
CERES	Clouds and the Earth's Radiant Energy System
CID	Cloud Imager Data (data product)
CRH	Clear Reflectance History (data product)
CRS	Clouds and Radiative Swath (data product)
CW	Cable Wrap
DAAC	Distributed Active Archive Center
DAC	Digital to Analog Converter
DAO	Data Assimilation Office
DAP	Data Acquisition microProcessor
DMA	Direct Memory Access
DMS	Data Management System
DPC	Data Products Catalog
ECR	Earth-Centered Rotating
EDDB	ERBE-Like Daily Database Product
EDOS	EOS Data Operations System
EOS	Earth Observing System
EOS AM	EOS Morning Crossing Mission (Renamed Terra)
EOS PM	EOS Afternoon Crossing Mission (Renamed Aqua)
EOSDIS	Earth Observing System Data and Information System
ERBE	Earth Radiation Budget Experiment
ERBS	Earth Radiation Budget Satellite
FAPS	Fixed Azimuth Plane Scan
FM	Flight Model
FOV	Field-of-View (See Term-6)
FSW	Monthly Single Satellite Fluxes and Clouds
FTP	File Transfer Protocol

GAP	Gridded Analysis Product
GB	Gigabyte
GEO	Geostationary Narrowband Radiances
GMS	Geostationary Meteorological Satellite
GGEO	Gridded Geostationary Narrowband Radiances
GMT	Greenwich Mean Time
GOES	Geostationary Operational Environmental Satellite
H	High
HDF	Hierarchical Data Format
IES	Instrument Earth Scans (data product)
IGBP	International Geosphere Biosphere Programme
INSTR	Instrument
ISCCP	International Satellite Cloud Climatology Project
IWC	Ice Water Content
LaRC	Langley Research Center
LaTIS	Langley TRMM Information System
L	Low
LM	Lower Middle
LW	Longwave
LWC	Liquid Water Content
MAM	Mirror Attenuator Mosaic
MB	Megabyte
METEOSAT	Meteorological Satellite
MISR	Multi-angle Imaging SpectroRadiometer
MLE	Maximum Likelihood Estimator
MOA	Meteorological, Ozone, and Aerosols (data product)
MODIS	Moderate Resolution Imaging Spectrometer
MWH	Microwave Humidity (data product)
NASA	National Aeronautics and Space Administration
NOAA	National Oceanic and Atmospheric Administration
OPD	Ozone Profile Data (data product)
PFM	Prototype Flight Model (on TRMM)
PSA	Product Specific Attribute
PSF	Point Spread Function (See Term-12)
QA	Quality Assessment
RAPS	Rotating Azimuth Plane Scan
SARB	Surface and Atmospheric Radiation Budget
SBUV-2	Solar Backscatter Ultraviolet/Version 2
SDS	Scientific Data Set (See Term-19)
SFC	Hourly Gridded Single Satellite TOA/Surface Fluxes and Clouds (data product)
SPS	Solar Presence Sensor

SRB	Surface Radiation Budget
SRBAVG	Surface Radiation Budget Average (data product)
SS	Subsystem
SSF	Single Satellite CERES Footprint TOA and Surface Fluxes, Clouds (data product)
SSM/I	Special Sensor Microwave/Imager
SURFMAP	Surface Map
SW	Shortwave
SWICS	Shortwave Internal Calibration Source
SYN	Synoptic Radiative Fluxes and Clouds
TBD	To Be Determined
TISA	Time Interpolation and Spatial Averaging
TMI	TRMM Microwave Imager
TOA	Top-of-the-Atmosphere (See Term-22)
TOT	Total
TRMM	Tropical Rainfall Measuring Mission
UM	Upper Middle
URL	Uniform Resource Locator
UT	Universal Time
UTC	Universal Time Code
VIRS	Visible Infrared Scanner
WN	Window
WWW	World Wide Web
ZAVG	Monthly Zonal and Global Average Radiative Fluxes and Clouds (data product)

16.2 CERES Units

Unit Definitions

Units	Definition
AU	Astronomical Unit
cm	centimeter
count	count, counts
day	day, Julian date
deg	degree
deg sec ⁻¹	degrees per second
du	Dobson units
fraction	fraction 0..1
g kg ⁻¹	gram per kilogram
g m ⁻²	gram per square meter
hhmmss	hour, minute, second
hour	hour
hPa	hectoPascals
in-oz	inch-ounce

Unit Definitions

Units	Definition
K	Kelvin
km	kilometer, kilometers
km sec ⁻¹	kilometers per second
m	meter
mA	milliamp, milliamps
micron	micrometer, micron
msec	millisecond
mW cm ⁻² sr ⁻¹ μm ⁻¹	milliWatts per square centimeter per steradian per micron
m sec ⁻¹	meter per second
N/A	not applicable, none, unitless, dimensionless
percent	percent, percentage 0..100
rad	radian
sec	second
volt	volt, volts
W h m ⁻²	Watt hour per square meter
W ² m ⁻⁴	square Watt per meter to the 4th
W m ⁻²	Watt per square meter
W m ⁻² sr ⁻¹	Watt per square meter per steradian
W m ⁻² sr ⁻¹ μm ⁻¹	Watt per square meter per steradian per micron
C	degrees centigrade
μm	micrometer, micron

17.0 Document Information

17.1 Document Creation Date - May 15, 1998

17.2 Document Review Date -

17.3 Document Revision Date

Month 1999 Comment

17.4 Document ID

LD_007_010_001_00_00_0_yyyymmdd

(Release Date) *[get this from ASDC User Services]*

17.5 Citation

Please provide a reference to the following paper when scientific results are published using the CERES XYZ TRMM data:

“Wielicki, B. A.; Barkstrom, B.R.; Harrison, E. F.; Lee III, R.B.; Smith, G.L.; and Cooper, J.E., 1996: Clouds and the Earth’s Radiant Energy System (CERES): An Earth Observing System Experiment, Bull. Amer. Meteor. Soc., 77, 853-868.”

When Langley Atmospheric Sciences Data Center (ASDC) data are used in a publication, the following acknowledgment is requested to be included:

“These data were obtained from the NASA Langley Research Center EOSDIS Distributed Active Archive Center.”

The Data Center at Langley requests two reprints of any published papers or reports which cite the use of data the Langley ASDC have distributed. This will help the ASDC to determine the use of data distributed, which is helpful in optimizing product development. It also helps the ASDC to keep product related references current.

17.6 Redistribution of Data

To assist the Langley ASDC in providing the best service to the scientific community, a notification is requested if these data are transmitted to other researchers.

17.7 Document Curator

The Langley ASDC Science, User & Data Services Office.

18.0 Index

Appendix A CERES Metadata

This section describes the metadata that are written to all CERES HDF products. [Table A-1](#) describes the CERES Baseline Header Metadata that are written on both HDF and binary direct access output science data products. The parameters are written in HDF structures for CERES HDF output products and are written as 80-byte records for binary direct access output products. Some parameters may be written in multiple records. [Table A-2](#) describes the CERES_metadata Vdata parameters which are a subset of the CERES Baseline Header Metadata and are also written to all CERES HDF output products. For details on CERES Metadata, see the CERES Software Bulletin “CERES Metadata Requirements for LaTIS” (Reference [11](#)).

[Table A-1](#) lists the item number, parameter name, units, range or allowable values, the data type, and the maximum number of elements. Note that there are two choices for parameters 22-25 and two choices for parameters 26-29. The choices depend on whether the product is described by a bounding rectangle or by a GRing. Abbreviations used in the Data Type field are defined as:

s =	string	date =	yyyy-mm-dd
F =	float	time =	hh:mm:ss.xxxxxxZ
I =	integer	datetime =	yyyy-mm-ddThh:mm:ss.xxxxxxZ

Table A-1. CERES Baseline Header Metadata

Item	Parameter Name	Units	Range	Data Type	No. of Elements
1	ShortName	N/A	N/A	s(8)	1
2	VersionID	N/A	0 .. 255	I3	1
3	CERPGEName	N/A	N/A	s(20)	1
4	SamplingStrategy	N/A	CERES, TRMM-PFM-VIRS, Terra-FM1-MODIS, TBD	s(20)	1
5	ProductionStrategy	N/A	Edition, Campaign, DiagnosticCase, PreFlight, TBD	s(20)	1
6	CERDataDateYear	N/A	1997 .. 2050	s(4)	1
7	CERDataDateMonth	N/A	1 .. 12	s(2)	1
8	CERDataDateDay	N/A	1 .. 31	s(2)	1
9	CERHrOfMonth	N/A	1 .. 744	s(3)	1
10	RangeBeginningDate	N/A	1997-11-19 .. 2050-12-31	date	1
11	RangeBeginningTime	N/A	00:00:00.000000Z .. 24:00:00.000000Z	time	1
12	RangeEndingDate	N/A	1997-11-19 .. 2050-12-31	date	1
13	RangeEndingTime	N/A	00:00:00.000000Z .. 24:00:00.000000Z	time	1
14	AssociatedPlatformShortName	N/A	TRMM, Terra, Aqua, TBD	s(20)	1-4
15	AssociatedInstrumentShortName	N/A	PFM, FM1, FM2, FM3, FM4, FM5, TBD	s(20)	1-4

Table A-1. CERES Baseline Header Metadata

Item	Parameter Name	Units	Range	Data Type	No. of Elements
16	LocalGranuleID	N/A	N/A	s(80)	1
17	PGEVersion	N/A	N/A	s(10)	1
18	CERProductionDateTime	N/A	N/A	datetime	1
19	LocalVersionID	N/A	N/A	s(60)	1
20	ProductGenerationLOC	N/A	SGI_xxx, TBD	s(255)	1
21	NumberOfRecords	N/A	1 .. 9 999 999 999	I10	1
22	WestBoundingCoordinate	deg	-180.0 .. 180.0	F11.6	1
23	NorthBoundingCoordinate	deg	-90.0 .. 90.0	F11.6	1
24	EastBoundingCoordinate	deg	-180.0 .. 180.0	F11.6	1
25	SouthBoundingCoordinate	deg	-90.0 .. 90.0	F11.6	1
22	GRingPointLatitude	deg	-90.0 .. 90.0	F11.6	5
23	GRingPointLongitude	deg	-180.0 .. 180.0	F11.6	5
24	GRingPointSequenceNo	N/A	0 .. 99999	I5	5
25	ExclusionGRingFlag	N/A	Y (= YES), N (= NO)	s(1)	1
26	CERWestBoundingCoordinate	deg	0.0 .. 360.0	F11.6	1
27	CERNorthBoundingCoordinate	deg	0.0 .. 180.0	F11.6	1
28	CEREastBoundingCoordinate	deg	0.0 .. 360.0	F11.6	1
29	CERSouthBoundingCoordinate	deg	0.0 .. 180.0	F11.6	1
26	CERGRingPointLatitude	deg	0.0 .. 180.0	F11.6	5
27	CERGRingPointLongitude	deg	0.0 .. 360.0	F11.6	5
28	GRingPointSequenceNo	N/A	0 .. 99999	I5	5
29	ExclusionGRingFlag	N/A	Y (= YES), N (= NO)	s(1)	1
30	AutomaticQualityFlag	N/A	Passed, Failed, or Suspect	s(64)	1
31	AutomaticQualityFlagExplanation	N/A	N/A	s(255)	1
32	QAGranuleFilename	N/A	N/A	s(255)	1
33	ValidationFilename	N/A	N/A	s(255)	1
34	ImagerShortName	N/A	VIRS, MODIS, TBD	s(20)	1
35	InputPointer	N/A	N/A	s(255)	800
36	NumberInputFiles	N/A	1 .. 9999	I4	1

Table A-2 describes the CERES_metadata Vdata parameters which are written to all CERES HDF output science products. The table lists the item number, parameter name, units, range or allowable values, and the parameter data type where s(x) denotes a string of x characters.

Table A-2. CERES_metadata Vdata

Item	Parameter Name	Units	Range	Data Type
1	ShortName	N/A	N/A	s(32)
2	RangeBeginningDate	N/A	1997-11-19 .. 2050-12-31	s(32)
3	RangeBeginningTime	N/A	00:00:00.000000Z .. 24:00:00.000000Z	s(32)
4	RangeEndingDate	N/A	1997-11-19 .. 2050-12-31	s(32)
5	RangeEndingTime	N/A	00:00:00.000000Z .. 24:00:00.000000Z	s(32)
6	AutomaticQualityFlag	N/A	Passed, Failed, or Suspect	s(64)
7	AutomaticQualityFlagExplanation	N/A	N/A	s(256)
8	AssociatedPlatformShortName	N/A	TRMM, Terra, Aqua, TBD	s(32)
9	AssociatedInstrumentShortName	N/A	PFM, FM1, FM2, FM3, FM4, FM5, TBD	s(32)
10	LocalGranuleID	N/A	N/A	s(96)
11	LocalVersionID	N/A	N/A	s(64)
12	CERProductionDateTime	N/A	N/A	s(32)
13	NumberOfRecords	N/A	1 .. 9 999 999 999	4-byte integer
14	ProductGenerationLOC	N/A	SGI_xxx, TBD	s(256)